Insights into C and H storage in the altered oceanic crust: Results from ODP/IODP Hole 1256D

S. Shilobreeva, I. Martinez, Vincent Busigny, P. Agrinier, C. Laverne

Insights into C and H storage in the altered oceanic crust: results from ODP/IODP Hole 1256D

S. Shilobreeva [a,b], I. Martinez [a], V. Busigny [a,c], P. Agrinier [a], C. Laverne [d]

[a] Lab de Géochimie des isotopes stables et Centre de Recherches sur le Stockage Géologique du CO_2, IPGP Sorbonne Paris Cité, 1 rue Jussieu, 75238 Paris cedex 05, France.

[b] Vernadsky Institute of Geochemistry and Analytical Chemistry of Russian Academy of Sciences, Moscow, Russia

[c] Lab de Géochimie et Cosmochimie, IPGP Sorbonne Paris Cité, 1 rue Jussieu, 75238 Paris cedex 05, France.

[d] Lab de Pétrologie magmatique, Case 441, Université Paul Cézanne Aix-Marseille III, Faculté des Sciences et Techniques, Avenue Escadrille Normandie Niemen, F-13397 Marseille Cedex 20.

Corresponding author. Isabelle Martinez, e-mail adress: martinez@ipgp.jussieu.fr

Revised for GCA

Components: 9,847 words in main text; 6 Figures; 6 Tables

Abstract: 431 words

Abstract

Carbon and hydrogen concentrations and isotopic compositions were measured in 19 samples from altered oceanic crust cored in ODP/IODP Hole 1256D through lavas, dikes down to the gabbroic rocks. Bulk water content varies from 0.32 to 2.14 wt% with δD values from -64 to -25‰. All samples are enriched in water relative to fresh basalts. The δD values are interpreted in terms of mixing between magmatic water and another source that can be either secondary hydrous minerals and/or H contained in organic compounds such as hydrocarbons. Total CO_2, extracted by step-heating technique, ranges between 564 and 2823 ppm with $\delta^{13}C$ values from -14.9‰ to -26.6‰. As for water, these altered samples are enriched in carbon relative to fresh basalts. The carbon isotope compositions are interpreted in terms of a mixing between two components: (1) a carbonate with $\delta^{13}C$ = -4.5‰ and (2) an organic compound with $\delta^{13}C$ = -26.6‰.A mixing model calculation indicates that, for most samples (17 of 19), more than 75% of the total C occurs as organic compounds while carbonates represent less than 25%. This result is also supported by independent estimates of carbonate content from CO_2 yield after H_3PO_4 attack. A comparison between the carbon concentration in our samples, seawater DIC (Dissolved Inorganic Carbon) and DOC (Dissolved Organic Carbon), and hydrothermal fluids suggests that CO_2 degassed from magmatic reservoirs is the main source of organic C addition to the crust during the alteration process. A reduction step of dissolved CO_2 is thus required, and can be either biologically mediated or not. Abiotic processes are necessary for the deeper part of the crust (>1000 mbsf) because alteration temperatures are greater than any hyperthermophilic living organism (i.e. T>110°C). Even if not required, we cannot rule out the contribution of microbial activity in the low-temperature alteration zones. We propose a two-step model for carbon cycling during crustal alteration: (1) when "fresh" oceanic crust forms at or close to ridge axis, alteration starts with hot hydrothermal fluids enriched in magmatic CO_2, leading to the formation of organic compounds during Fischer-Tropsch-type reactions; (2) when the crust moves away from the ridge axis, these interactions with hot hydrothermal fluids decrease and are replaced by seawater interactions with carbonate precipitation in fractures. Taking into account this organic carbon, we estimate C isotope composition of mean altered oceanic crust at ~ -4.7‰, similar to the $\delta^{13}C$ of the C degassed from the mantle at ridge axis, and discuss the global carbon budget. The total flux of C stored in the altered oceanic crust, as carbonate and organic compound, is $2.9\pm0.4 \times 10^{12}$ molC/yr.

1. INTRODUCTION

Volatile elements such as C and H are studied in rocks since they control many geological processes ranging from mantle melting to Earth's climate and origin of life. The global geochemical cycles of volatile elements are dominated by exchanges between mantle and exosphere (i.e. atmosphere, hydrosphere and crust) through volcanic and subduction activities (e.g. Javoy, 1998). In detail, the generation, alteration and recycling of the oceanic crust represent the main geodynamic vector of exchanges between mantle and surface reservoirs. The alteration of oceanic crust on the seafloor, and its subsequent metamorphism in subduction zones have a major impact on the chemical composition of the material ultimately recycled to the deep mantle (e.g. Gregory and Taylor, 1981; Muehlenbachs, 1986; Valley, 1986; Bebout, 1995; Shanks et al., 1995; Bach et al., 2003). Over the past decades, stable isotopes systematic (C, H but also O, N and S) have been widely used to understand physico-chemical processes associated with alteration of oceanic crust. Various questions have been addressed such as volatile element speciation in altered rocks, chemical changes of the rock and fluid during alteration, water-rock ratios, alteration temperature, or fluid source and origin (e.g. Alt et al., 1986, 1996; Kawahata et al., 1987; Agrinier et al. 1995a, 1995b; Charlou et al., 1996; Teagle et al., 1998; Bach et al., 2001; Busigny et al., 2005; Li et al., 2007; Delacour et al., 2008).

Although it is largely accepted that volatile elements are incorporated into the oceanic crust during alteration with seawater and/or hydrothermal fluids, the flux and speciation of carbon involved in this transfer remains poorly known (e.g. Alt and Teagle, 1999; Staudigel, 2007; Delacour et al., 2008). Particularly, it is not known whether condensed carbon-rich phases may form during seawater-crust interactions. The detailed study of altered rocks is a key to better constrain the fate of C during alteration. Another interest for studying C geochemical behavior and fluxes during alteration of oceanic crust is that CO_2-rich water circulation into the crust may be considered as a natural analogue for CO_2 storage in basaltic rocks. Indeed, fresh basalts forming the oceanic crust have low carbon concentration (given an average value for glasses of 266 ppm CO_2; Mattey et al., 1984; Sakai et al.,1984; Pineau and Javoy, 1994; Pineau et al., 2004; Aubaud et al., 2004), whereas seawater, responsible for hydrothermal alteration of this crust, is relatively rich in CO_2 (2 mM in seawater; e.g. Bauer et al., 1998). Water-rock interactions of such system are heavily explored from both experiments

and thermodynamic modelling, but studies on natural samples are still missing while they could illustrate long-term reactions.

In the present contribution, we analyzed simultaneously concentration and isotopic composition of C and H in altered basalts and gabbros cored in Ocean Drilling Program/Integrated Ocean Drilling Program (ODP/IODP) Hole 1256D. Hole 1256D is quite unique since it is the first drill hole to penetrate a continuous section into the deepest part of the oceanic crust, i.e. the gabbroic section (Wilson et al., 2006). Accordingly, the present study is the first to investigate chemical and isotopic variations of volatiles along a vertical profile of in-situ oceanic crust from the lavas, through the sheeted dike complex, down to the gabbros. The coupling approach between C and H isotopes is used to evaluate (i) qualitatively their geochemical behavior during fluid-rock interactions and (ii) quantitatively constrain their exchange fluxes between seawater and oceanic crust. It provides new insights into these reactions as well as the nature of the carbon sources in bulk rocks from basaltic oceanic crust, away from veins.

2. GEOLOGICAL SETTING AND SAMPLING

2.1. Geological setting

Ocean Drilling Program Hole 1256D (6°44.2'N, 91°56.1'W) is located on the eastern flank of the East Pacific Rise (Figure 1). It lies on ~15 Ma oceanic lithosphere of the Cocos plate under 3635 m of water in the Guatemala oceanic basin. ODP Hole 1256D has been chosen in the hope to drill a complete section of oceanic crust because the crust at this site was accreted at a superfast spreading rate (~200-220 mm/yr; Wilson, 1996) and the upper gabbros were predicted to occur at relatively shallow depth (1100-1300 mbsf; Shipboard Scientific Party, 2003). Hole 1256D was initiated in 2002 during Ocean Drilling Program Leg 206 (Shipboard Scientific Party, 2003). In 2005, Integrated Ocean Drilling Program Expeditions 309 and 312 successfully deepened Hole 1256D, allowing for the first time to reach gabbros along a continuous section of upper oceanic basement (Wilson et al., 2006). ODP/IODP Hole 1256D reaches a depth of 1507.1 mbsf (meters below seafloor).

2.2. Lithostratigraphy and alteration of Hole 1256D

The lithostratigraphy and alteration of the crust drilled in Hole 1256D are detailed in Teagle et al. (2006). They are summarized below. The lithostratigraphy of Hole 1256D shows 6 main units: (1) from 0 to 250 mbsf, a sediment blanket; (2) from 250 to 534 mbsf, a pile of volcanics interpreted as being emplaced off-axis, composed of a ~100-m-thick sequence of lava dominated by a single flow, up to 75 m thick (lava pond), overlying inflated lava flows (Umino et al., 2000); (3) from 534 to 1004 mbsf, lavas that erupted at the ridge axis, composed of sheet flows, massive flows and minor pillow lavas; (4) from 1004 to 1061 mbsf, lithologic transition zone marked by subvertical intrusive contacts and mineralized breccias ; (5) from 1061 to 1407 mbsf, relatively thin sheeted dike complex (some basalts have doleritic textures, and many are cut by subvertical dikes with common strongly brecciated and mineralized chilled margins); (6) from 1407 to 1507 mbsf, plutonic complex, composed of two major bodies of gabbro, intrusive into dikes, with a 52-m-thick upper gabbro separated from a 24-m thick lower gabbro by a 24-m screen of granoblastic dikes.

The main alteration features of the oceanic crust penetrated by Hole 1256D are reported in Table 1 and can be summarized as follow. Similarly to other drill holes, the volcanic section has been altered at low temperature (<150°C). Alteration by oxidizing seawater is much less common than in Hole 504B (Alt, 1995, Alt et al., 2010) but similar to other fast spreading crust (Alt and Teagle, 2003). The conditions were generally reducing (as attested by smectite as the main secondary phase of the background alteration) except in alteration halos adjacent to iron oxyhydroxides-bearing veins. There is a stepwise increase in alteration grade downward from lavas into dikes, that are partially altered to chlorite and other greenschist facies minerals at temperatures greater than ~250°C. Within the dikes the grade and intensity of this hydrothermal alteration increase downward, with actinolite more abundant than chlorite below 1300 mbsf and with hornblende present below 1350 mbsf, indicating temperatures approaching ~400°C. The dikes have significantly lower porosity (mostly 0.5–2%) than the volcanic section (2-10%). In the lower 60 m of the sheeted dikes (1348 to 1407 mbsf), basalts are partially to completely recrystallized to distinctive granoblastic textures resulting from contact metamorphism by underlying gabbroic intrusions (Koepke et al., 2008; France et al., 2009). Both upper and lower gabbros are moderately to highly altered by hydrothermal fluids to actinolitic hornblende, secondary plagioclase, epidote, chlorite, prehnite, and laumontite. The intensity of hydrothermal alteration increases with grain size and proximity to intrusive boundaries. Porosity increases stepwise downward from lowermost dikes (0.1-0.3%) into the uppermost gabbro (1.0-2.2%), as the result of the

contact metamorphism of the granoblastic dikes and the strong hydrothermal alteration of the uppermost gabbros. In the lower gabbros, porosity is then slightly lower (0.5-2%).

2.3. Samples description

In order to represent the various lithostratigraphic (lava, lava/dike transition, sheeted dikes, gabbros) and alteration (low temperature, transition, hydrothermal alteration, granoblastic) types, nineteen rock samples have been selected as regularly as possible downhole (Table 1). We analyzed mostly background alteration samples, while veins and alteration halos adjacent to veins were generally avoided. Only one carbonate-bearing vein was analyzed in order to represent pure carbonate endmember (sample 149). In samples 16, 66 and 150, different parts were analyzed: one representing the background alteration (samples 16b, 150b), the individual halo (66a) or background alteration associated with halo (samples 16a, 66b, 150a).

Samples altered at low temperature (6, 16, 37, 52; Table 1) are composed mainly by primary unaltered clinopyroxene and plagioclase. Secondary minerals occur in vesicles and interstitial areas. Smectite is the dominant secondary mineral of the background rock, whereas some amounts of Fe-oxyhydroxides and celadonite occur in an alteration halo (sample 16a) adjacent to a Fe-oxyhydroxides + celadonite vein. Samples altered in conditions transitional between low temperature and hydrothermal (66, 87, 102) present alteration features similar to those described above, except the presence of minor amounts of hydroschorlomite in samples 66b and 102, and the presence of smectite/chlorite and vermiculite/chlorite mixtures instead of smectite (Laverne et al. 2006). In samples affected by hydrothermal alteration (123 to 231) primary phases are partly or completely replaced by greenschist facies minerals (Table 1). Deeper samples (196, 207, 227) show the effects of both hydrothermal alteration and granoblastic recrystallization. The latter is characterized by an assemblage of small rounded crystals of plagioclase, clinopyroxene and orthopyroxene (Teagle et al., 2006; Koepke et al., 2008). No carbonates were observed optically in the various studied samples, except in a vein in sample 150 (but this vein was not analyzed, neither in 150a, nor in 150b) and in the vein of sample 149. Chemical compositions of representative secondary minerals of samples analyzed in this study are reported in Table 2.

3. ANALYTICAL METHOD

3.1. Step heating extraction

Step-heating experiments (Javoy and Pineau, 1991; Pineau and Javoy, 1994) have been used for volatile extraction (CO_2 and H_2O) from silicate powders. Samples were crushed, sieved to fraction <150 μm and homogeneized. About 200 mg of powder were loaded in a quartz tube and connected to a vacuum line. Step heating of the sample was obtained using a vertical cylindrical furnace, with temperature stability of ±1-2°C. The main advantage of the step heating technique is that it provides some means to differentiate various sources of carbon, such as carbonate and reduced carbon phases that include non-carbonate carbon such as graphite and various organic compounds *sensu stricto*. Hereafter we will use the term "organic" for non-carbonate C. For every sample, the following procedure was used: after one night degassing at room temperature, the samples were heated at 100°C during 1 hour to remove surface contaminants (water and other adsorbed compounds). Then the volatiles were extracted using 4 sequential steps: (1) heating at 250°C during 1 hour with 4 mbar partial pressure of O_2 to oxidize some organic components, (2) then heating at 900°C during 1 hour to extract CO_2 from carbonates. For this step, a little oxygen gas pressure (5×10^{-4} mbar) in the line was provided to guarantee complete oxidation of CO also produced during decarbonation. In our samples, which contain high water concentration, we noticed however that organic compounds could also be extracted at this step because oxygen fugacity is raised. (3) The samples were heated at 1170°C during 1 hour to ensure complete decarbonation (still with $5x10^{-4}$ mbar of O_2) and (4) the oxygen pressure was then raised up to 4 mbar, while the sample was maintained at 1170°C during 30 minutes, in order to oxidize all the reduced carbon phases (e.g. graphite). For steps (2), (3) and (4), gases were extracted dynamically using liquid nitrogen trap. After each step, gaseous CO_2 and H_2O were cryogenically separated and collected. CO_2 was quantified by Baratron® or with a Toepler pressure gauge, with a precision better than 5%. Mean blank values are 15, 33, 29 and 46 ppm CO_2 for the 250°C, 900°C, 1170°C without O_2 and 1170°C with O_2 steps, respectively.

Total accumulated water released during the four temperature steps, was converted to H_2 by reaction with hot uranium (800°C) and the H_2 yield was measured manometrically with a Toepler pump. To report D/H ratios of water versus V-SMOW scale, the hot uranium has been calibrated using a set of three waters calibrated versus SMOW and NBS30 biotite. For sample 123, volatile extractions was performed twice in order to test reproducibility and

sample homogeneity (see Table 3). Blank measurements were carried out using the step heating experimental protocol described above and corrections were made on all the data reported in Table 3.

3.2. H_3PO_4 acid attack

In order to determine the carbonate content, approximately 200 mg of rock powder were loaded in quartz tube and reacted under vacuum with 100% H_3PO_4 acid for 3 hours at 80°C to extract CO_2 from carbonates (McCrea, 1950). CO_2 was then collected, purified to remove trace of water and quantified by Baratron® pressure gauge, giving a precision better than 5%. Blank measurements were carried out using the same experimental protocol and found to be 0.01 μmol CO_2 (i.e. about 3 ppm of CO_2 when compare to sample weight).

3.3. Carbon and hydrogen isotope analyses

The isotopic ratios have been measured on a Thermofisher Delta +XP and Mat 253. They are reported in Table 3 using the conventional δ notation vs V-SMOW for hydrogen isotopes and vs. PDB for carbon isotopes. For H_2, the H_3^+ interference factor was estimated before any hydrogen isotope measurements. The external repeatability of hydrogen isotopic measurement is about ± 2 ‰ (2σ). Repeated measurements of the international graphite standard USGS24 gave $\delta^{13}C$ values of -15.96 ± 0.06 ‰ (2σ; n=10). This value is indistinguishable from the recommanded value (-15.99 ± 0.11 ‰ 2σ; Stichler, 1995). Thus, the accuracy of the present procedure on $\delta^{13}C$ measurements is better than ±0.1‰ (2σ).

4. RESULTS

The amounts of water and carbon (as CO_2) extracted from the samples are listed in Table 3, as well as the corresponding δD and $\delta^{13}C$. For carbon, the proportion extracted at each of the four steps of the procedure is also displayed in Figure 2. Sample 123 was run twice giving a good reproducibility for both carbon and water estimates via this step heating methodology. In samples 16, 66 and 150, where three different alteration types were analyzed (i.e. background alteration, individual halo and background alteration associated with halo),

no clear difference in terms of volatile concentrations or isotopic composition could be evidenced. Sample 150, however, shows a significant enrichment in both water and CO_2 concentrations in the background alteration associated with halo (150a) relative to the background alteration sample (150b).

4.1 Carbon concentration and isotopic composition

For the 250°C step, all the samples but two yield significant amount of CO_2 (i.e. 3 times larger than the blank level); between 1 to 20 wt% of total CO_2 is recovered at this step. For the 900°C step, all the samples yield significant amount of CO_2, which represents more than 60 % of total CO_2 (Figure 2). For the 1170°C step without O_2, a few samples yield significant amount of CO_2, representing less than 20 % of total CO_2. At the 1170°C step with O_2, all the samples yield CO_2 amount at the blank level, showing that essentially all the carbon of the samples has been released by the 3 previous steps. Low temperature step (i.e. 250°C) may be compromised by the addition of adsorbed atmospheric volatiles and/or organic contaminant introduced after collection of the samples (Mattey et al., 1984; Sakai et al., 1984; Marty and Zimmermann, 1999). However, the large variation in $\delta^{13}C$ observed for this step may indicate that this carbon is not derived from contamination (i.e. contamination may give similar $\delta^{13}C$ values for all samples). This point is still a matter of debate but has only a little consequence in the case of Hole 1256D samples because the amount of CO_2 released at this step is always less than 20 % of the total carbon of the sample. In the following discussion, the total carbon concentration and isotopic composition will not include the 250°C step. Whether it is or not included does not change significantly the value of the total amount of CO_2, nor its $\delta^{13}C$ (see Table 3).

Sample 149, which contains a vein of carbonate, yields a high amount of CO_2 (34254 ppm CO_2) mainly released at the 900°C step. For all other samples, the total C content varies from 564 to 2823 ppm CO_2. The lowest C contents are observed for the deepest samples, where alteration occurred at low water-rock ratios and higher temperatures (Figure 3 and Table 3). The $\delta^{13}C$ values show a large variation range between -26.6‰ to -10.9‰. The $\delta^{13}C$ values are slightly increasing with depth, with the most negative value closer to the surface (see Figure 3).

Six samples were reacted with H_3PO_4 (Table 4). In all samples except 149, carbonate content was found to be very low (i.e. less than 200 ppm CO_2). This low amount of extracted

299 CO_2 limited our determination of C isotope composition to only one sample ($\delta^{13}C$ = -15.2‰).
300 Sample 149, containing a carbonate vein, has a much higher carbon content and $\delta^{13}C$ value (-
301 4.5‰), similar to that of carbonate veins analyzed in shallow part of Hole 1256D (Coggon et
302 al., 2006). Generally carbonate content determined by acid attack is significantly smaller than
303 total carbon determined by the step-heating extraction, about 20 % or less, thus indicating that
304 non-carbonate carbon represents most of the carbon in these samples.
305
306 **4.2 Water concentration and hydrogen isotope composition**
307
308 The amount of water extracted from the samples also shows a large variation from 0.32
309 to 3 wt% (Table 3). The sheeted dike complex is significantly enriched in water (> 1.57 wt%)
310 relative to other parts of the section. The δD values range from -25.1 to -64.2 ‰, with a slight
311 increase with depth from the top of the volcanic section to the transition zone.
312
313 **5. DISCUSSION**
314
315 **5.1. Origin and speciation of carbon and hydrogen in the altered oceanic crust**
316
317 The origin and speciation of C and H in the oceanic crust are important questions
318 because it may help to (i) quantify exchange between seawater and oceanic lithosphere and
319 (ii) deduce the later fate of these elements in subduction environment. Carbon and hydrogen
320 in the altered oceanic crust may either be inherited from magmatic processes or be derived
321 from seawater-rock interaction.
322
323 *5.1.1. Carbon signature: a mixing between oxidized and reduced compounds*
324
325 Altered rocks from Hole 1256D have a bulk-rock carbon content from 564 to 2823
326 ppm CO_2 (average 1389 ppm CO_2) and $\delta^{13}C$ range from -10.9 to -26.6 ‰ with mean value of
327 -22 ± 2‰ (1σ). In comparison, fresh basalt glasses from mid-ocean ridges have carbon
328 content from 44 to 613 ppm CO_2 (average 266 ppm CO_2; n=37) and $\delta^{13}C$ range from -12.2 to
329 -5.3 ‰, except two values at ~ -24.5‰ (Figure 4 and references therein). Accordingly, data
330 from Hole 1256D show an enrichment in C content with light isotopic signature relative to
331 fresh basalts. Contrasting with water-bearing phases that may be directly identified from

petrological observations on thin-section, the determination of carbon speciation is not straightforward and mostly relies on C isotope analyses. In the oceanic crust, carbon can occur in several phases either as oxidized or reduced compounds. Oxidized phases include carbonates precipitating from dissolved inorganic carbon (DIC) in seawater (marine carbonate); carbonates from microbially altered volcanic glasses (Furnes et al., 2001; Banerjee et al., 2004) as well as CO_2 in vesicles and fluid inclusions (Pineau et al., 2004). Reduced forms may include graphite, organic carbon (Tingle et al., 1991) and reduced carbon gases such as methane trapped in bubbles and fluid inclusions (Charlou et al., 1996; Kelley and Früh-Green, 2001). However in samples from Hole 1256D, fluid inclusions and bubbles are rare, except for some quartz veins in the sheeted dikes and gabbros, and represent a negligible amount of the total carbon at least in the analyzed samples. From an equilibrium isotopic point of view, the reduced C phases (e.g. graphite, hydrocarbon) generally tend to be depleted in the heavy isotope relative to the oxidized phases (carbonates and CO_2) (Bottinga, 1969; Des Marais et al., 1992). Oceanic crust carbonates occurring in veins usually have carbon isotope composition between -3 and +3 ‰ (Coggon et al., 2006). Recently, however, carbonates associated with microbially altered volcanic glasses have shown larger variations with $\delta^{13}C$ ranging from -16‰ up to +5% (Furnes et al., 2001). In contrast, reduced C phases in oceanic rocks have lower $\delta^{13}C$ around -25‰. For instance, Delacour et al. (2008) reported $\delta^{13}C$ values for total organic carbon (TOC) ranging from -28.9 to -21.5‰ in serpentinized peridotites and gabbroic rocks from Lost City Hydrothermal System (Mid-Atlantic Ridge). In these rocks, it was suggested that total carbon is a mixture of organic carbon and carbonates of marine origin (Delacour et al., 2008). Likewise, the range of C isotope composition observed in our samples (-14.9 to -26.6 ‰) can only be explained by the presence of reduced C phase together with carbonate in relatively minor amounts. As the graphite stability field (above 600°C; Libera and Gogotsi, 2001) was probably not reached, except for few samples from the plutonic zone where hydrothermal metamorphism occurred at temperatures as high as 900°-950°C (Koepke et al., 2008; Alt et al., 2010), it is not reasonable to invoke the contribution of graphite in these samples. We derive consequently that most of carbon occurs as “organic compounds” which have not necessarily a biogenic origin.

On the basis of the carbon isotope balance, an evaluation of the fraction of carbonate (carb) and organic compound (OC) present in each sample can be calculated using:

$$\delta^{13}C_{tot} = n\,\delta^{13}C_{OC} + (1-n)\delta^{13}C_{carb} \qquad (1)$$

where $\delta^{13}C_{tot}$ corresponds to the measured isotope composition of total carbon (as CO_2), $\delta^{13}C_{OC}$ and $\delta^{13}C_{carb}$ being the isotopic composition of organic compound and carbonate, respectively; and n being the mole fraction of organic compound, i.e. $n = C_{OC}/C_{tot}$. In order to estimate a value for n, and as $\delta^{13}C_{tot}$ is the only measured isotopic composition, we assigned the most likely values to $\delta^{13}C_{OC}$ and $\delta^{13}C_{carb}$. For $\delta^{13}C_{carb}$ we considered two possible values: (1) $\delta^{13}C_{carb}$ = -4.5‰ which was measured using H_3PO_4 attack on a carbonate vein (sample 149) and (2) $\delta^{13}C_{carb}$ = 0.4‰, the average value obtained by Coggon et al. (2006) on 37 carbonates veins from the same drilling hole. For $\delta^{13}C_{OC}$, we considered the lowest value measured in the present sample set (-26.6‰). This value was also confirmed after analysis by step heating on sample 123 which was previously cleaned with HCl to remove carbonates. In this case, CO_2 obtained only comes from organic compounds: a $\delta^{13}C$ value of -25.7‰ was measured. Table 5 gives the mol fraction "n" of organic compound (i.e. C_{OC}/C_{tot}) calculated for the two different carbonate end-members and $\delta^{13}C_{OC}$ of -26.6‰. The C_{OC}/C_{tot} ratio varies from 0.47 to 1 (Table 5). Among all samples, only two (150a and 220) have as much carbonates as organic compounds ($C_{OC}/C_{tot} \approx 0.5$). All other samples (n=16) have C_{OC}/C_{tot} between 0.74 and 1, indicating that more than 74% of the total C occur as organic compounds. This result using the isotope balance approach is consistent with the comparison between the CO_2 yield after H_3PO_4 attack (Table 4) and that of the total carbon (Table 3).

In a recent study of serpentinized peridotites and gabbroic rocks from Mid-Atlantic Ridge, Delacour et al. (2008) interpreted reduced carbon as organic compounds mainly from marine biogenic origin. Gas chromatography allowed the authors to identify saturated hydrocarbons, mostly as n-alkanes ranging from C15 to C30. The nature and origin of an organic carbon is still an open question for samples from Hole 1256D. Several hypotheses can be considered: (1) direct incorporation of dissolved organic carbon (DOC) from seawater into altered basalts, (2) biotic reduction of dissolved inorganic carbon (DIC) from seawater, (3) abiotic reduction of DIC from seawater via Fischer-Tropsch reactions, or (4) incorporation and reduction of magmatic carbon dissolved in hydrothermal fluid.

These different scenarios can be tested if we determine the total amount of fluid interacting with our rock samples (i.e. water-rock ratio) and assuming that all DIC and/or DOC of the fluid is incorporated into the rock. The lavas from volcanic section interacted with seawater solutions so we assume seawater O, Sr and DIC compositions are representative of the fluid endmember. Using traditional methods based on Sr and O isotopes (e.g. Taylor, 1978; McCulloch et al., 1981) and database available for Hole 1256D (Harris et al., 2008), we

397 estimated the seawater-rock ratio of our samples to be lower than 5 for all samples. A very
398 good agreement between independent O and Sr methods was observed for this calculation.
399 Deep seawater DIC and DOC concentrations are respectively ~2400 and 40 µM (Bauer et al.,
400 1998; Hansel and Carlson, 1998). Considering deep seawater infiltration through the oceanic
401 crust, with a seawater-rock ratio of 5 and a total precipitation/fixation of C from fluid to the
402 rock, the gain of C to the rock would be ~2.4 ppm from DOC and ~144 ppm from DIC.
403 Because altered basalts from the volcanic section in ODP Hole 1256D show an increase in C
404 concentration of the order of 1000 ppm, we conclude that C provided to the rock from the
405 fluid does not derive dominantly from seawater (either as DOC or DIC). Another source of
406 carbon is required. Residual magmatic carbon, occurring as reduced carbon, is not expected to
407 be a significant source of C since it represents a maximum of ~200 ppm CO_2 (e.g. Pineau et
408 al., 2004). The most likely source is magmatic C degassing and diffusing through the crust
409 mixed with or dissolved into hydrothermal fluid. This hypothesis is supported by East Pacific
410 Rise hydrothermal fluids whose dissolved CO_2 (DIC) concentration can be as high as 200,000
411 µM and $\delta^{13}C_{DIC}$ similar to that of fresh MORBs ($\delta^{13}C$ between -1.9 to -7.9‰) interpreted to
412 be of magmatic origin (Charlou et al., 1996; Proskurowski et al., 2008). Comparatively, CH_4
413 concentrations in EPR hydrothermal fluids are much lower than CO_2 and can be neglected
414 (Charlou et al., 1996; Proskurowski et al., 2008). In the deep part of the crust, rocks (i.e. dikes
415 and gabbros) interacted with hydrothermal fluids, which are highly reacted seawater
416 solutions. The rocks and vent fluids integrate the effects of fluid-rock interaction over a range
417 of conditions, but an endmember calculation can be made using the Sr and O isotope
418 composition of hydrothermal vent fluids. The ratio $^{87}Sr/^{86}Sr$ and $\delta^{18}O$ value of hydrothermal
419 fluids released at ridge axis from East Pacific Rise are on average ~0.7041 and +1‰, with
420 limited range of variation (Shanks et al., 1995; Ravizza et al., 2001). Using these parameters
421 and the data for Hole 1256D (Harris et al., 2008), fluid-rock ratios lower than 4 are obtained
422 from O isotopes, while those obtained from Sr isotopes are between 6 and 200. The apparent
423 discrepancy between calculations from O and Sr may result from the temperature effect on O
424 isotope fractionation since it is not taken into consideration in the models (McCulloch et al.,
425 1981). Fluid-rock ratios calculated from Sr isotopes are likely more reliable because Sr does
426 not depend on temperature. Assuming that all the CO_2 dissolved in hydrothermal fluid
427 (200,000 µM ; Charlou et al., 1996; Proskurowski et al., 2008) is transferred to the rock
428 during alteration, the C concentration of the rock is increased by ~48,000 ppm for a
429 hydrothermal fluid-rock ratio of 200. This C concentration is 30 times higher than the one
430 required to explain the enrichment observed in our dike and gabbro samples, thus showing

that only a limited part of the total C is transferred from the fluid to the rock. In addition, the total transfer of carbon from the hydrothermal fluid to the rock would generate a C phase with $\delta^{13}C$ between -1.9 and -7.9 ‰ which is not the case since the samples $\delta^{13}C$ are all below -17 ‰. This contrast shows that a C isotope fractionation occurred. The invoked C fractionation must be in favor of an enrichment of ^{12}C in the organic carbon, which conforms to the theoretical partition of C isotope among oxidized and reduced carbon phases. To conclude, while $\delta^{13}C$ values measured in our samples suggest that C occurs mostly as organic compounds, a comparison between the C concentrations in our samples, seawater DIC and DOC, and hydrothermal fluids suggests that CO_2 degassed from magmatic reservoirs is likely the main source of CO_2 addition during alteration process. A reduction step of dissolved CO_2 is thus required, and can be either biologically mediated or not as will be discussed in part 5.3.

5.1.2. Hydrogen signature: from magmatic to secondary phases

Like for carbon, hydrogen in altered oceanic crust can be either derived from magmatic source or seawater. A compilation of bulk hydrogen analyzes in fresh degassed MORB glasses and phenocrysts show water content from 0.12 to 0.52 wt% (average of 0.25 ± 0.09 wt%, 1σ; n = 47) and δD values from -51 to -102 ‰ (average of -72.3 ± 9.9 ‰, 1 σ; n = 47) (Figure 5; Craig and Lupton, 1976; Kyser and O'Neil, 1984; Pineau et al., 2004). Altered rocks from Hole 1256D have water content and δD values higher than the range defined by fresh MORB, with some overlaps for few samples (see Figure 5). This confirms that alteration of upper oceanic crust increases water content of the rocks as observed previously (e.g. Kawahata et al., 1987; Agrinier et al., 1995a, 1995b; Alt, 2003). The high δD values relative to fresh MORB are similar to those observed in other sites of the oceanic crust (Kawahata et al., 1987; Agrinier et al., 1995a, 1995b; Javoy and Fouillac, 1979). However, it must be noted that other studies found δD values in the upper oceanic crust (i.e. volcanic section) lower than those of fresh MORB, with δD down to -170‰ (Hoernes and Friedrichsen, 1978; Friedrichsen and Hoernes, 1979; Friedrichsen, 1985; Alt, 2003). The apparent discrepancy between these data may arise either from (i) analytical problems (e.g. incomplete and fractionated H isotope extraction) or (ii) heterogeneity of the upper oceanic crust because different mineral phases can carry variable isotope signatures. This point will need to be clarified in a near future by separating and analyzing individual mineral phases.

In the rocks of the present study, water is added either as OH or H_2O in secondary minerals such as smectite, celadonite and Fe-oxyhydroxides at low temperature of alteration (T < 150°C), and chlorite, amphibole, epidote, prehnite and zeolite under hydrothermal alteration (T > 250°C). Water can also occur in fluid inclusions trapped in newly formed minerals (Vanko, 1988). However, petrological observation of the samples analyzed in the present study indicates that fluid inclusions represent a negligible amount of the total water. We can thus consider that water in samples from Hole 1256D should represent a mixing between inherited/primary magmatic water and secondary H-bearing minerals. In a δD-H_2O diagram (Figure 5), samples from Hole 1256D plot along a curved trend typical of a mixing relationship between two end-members. The first end-member can be identified as fresh MORB and the second one shows a range of δD between -20 and -40‰, with water content up to ~10 wt%, which corresponds typically to hydrous minerals. Petrological study of the present samples set indicates that OH or H_2O-bearing secondary minerals are on a first order smectite in the upper part of the section, then chlorite, and amphibole ± chlorite in the deeper part. At the temperatures of alteration (Table 1), hydrogen isotope fractionation between a fluid and these secondary minerals is around -30 ±10 ‰ (Graham et al., 1984, 1987; Hyeong and Capuano, 2004; Capuano, 1992; Chacko et al., 2001). Assuming that the fluid has seawater H isotope composition (i.e. δD = 0‰), the secondary minerals should be characterized by δD values around -30±10 ‰, similar to the δD values of the end-member deduced from Figure 5. This observation supports the hypothesis that hydrogen content and isotopic composition correspond to a mixing between a magmatic component and secondary H-bearing minerals. However, in the present contribution, we analyzed hydrogen content and isotopic composition in bulk rock and this hydrogen may not be derived only from H-bearing minerals. For instance, if organic compounds such as hydrocarbon are present, H linked to C can be released during step heating and analyzed in the bulk sample gas as well. The potential proportion of H derived from organic compounds can be estimated from the amount of C calculated using the model described above (see equation 1). The predominant types of hydrocarbons forming through alteration of oceanic crust are alkanes (Kelley and Früh-Green, 1999; Charlou et al., 1996, 2000; Delacour et al., 2008) and are defined by the general formula C_nH_{2n+2}. Since C/H molar ratio of alkanes varies in a well-defined range from 0.25 for methane to ~0.5 for heaviest alkanes, the concentration of H (in mol/g) derived from organic compounds can be calculated as:

$$H_{OC} = \frac{C_{OC}}{(C/H)_{alkane}} = \frac{n \times C_{tot}}{(C/H)_{alkane}} \qquad (2)$$

where C_{OC} is the organic C content (in mol/g), $(C/H)_{alkane}$ is the C/H molar ratio of alkanes, n is the molar fraction of organic C, and C_{tot} is the total C concentration measured in the sample (in mol/g). The molar fraction of H present as hydrocarbon can then be calculated from,

$$X_{(H)_{OC}} = \frac{H_{OC}}{H_{tot}} \quad (3)$$

where H_{tot} is the total H concentration measured in the sample by bulk extraction. From equation (1), (2) and (3), we have estimated the maximum molar fraction of H possibly present in organic compounds. The results are given in Table 5. Samples in the deeper part (depth > 1000 mbsf) all have H_{OC}/H_{tot} lower than 10%, indicating a negligible amount of H derived from organic compounds. In contrast, samples from the shallowest part (< 1000 mbsf) have H_{OC}/H_{tot} ratios higher than 10%, with values up to 33% (sample 16b). This larger proportion of hydrocarbon is also compatible with the observed variation in the $\delta^{13}C$ values, being more negative in the shallower part of the sections. This significant proportion of H from organic compounds may partly explain the negative δD values measured in samples from the shallowest part because hydrocarbons formed during oceanic crust alteration have very negative δD values (i.e. < -123‰; Welhan and Lupton, 1987). A plot of the measured δD values versus calculated H_{OC}/H_{tot} ratio (not shown) displays a rough negative trend, which is not statistically significant ($r^2 = 0.433$). This indicates that negative δD values observed in samples from Hole 1256D cannot be explained only by the contribution of hydrocarbons but also require the presence of inherited magmatic component. To summarize, H extracted from the present sample set is interpreted as a mixing between (1) OH/H_2O bearing minerals formed by interaction with seawater, (2) H derived from secondary hydrocarbons (such as alkanes) and (3) a residual primary magmatic component.

5.2. Physico-chemical conditions and spatial distribution of oceanic crust alteration at Hole 1256D

Carbon and hydrogen contents and isotopic composition can be useful to reconstruct the physico-chemical conditions of oceanic crust alteration at Hole 1256D. The dominance of an organic carbon component over carbonates in the host rocks suggests a reducing environment where the system was mostly buffered by the rock but not by a fluid during alteration. Low water-rock ratio of the volcanic zone (lava pond + inflated flows + sheet and

massive flows) is also supported by the low degree of alteration (typically ~10%; Teagle et al., 2006; Alt et al., 2010), as reflected herein by petrology and low water content (only slightly higher than fresh MORB). In contrast, the transition zone and the sheeted dike complex (from 1030 to 1330 mbsf) show significant enrichment in water, indicating a higher degree of alteration (~40%; Teagle et al., 2006; Alt et al., 2010). This spatial distribution of alteration is in good agreement with results from other geochemical studies (e.g. Sr, O and U), showing contrasting behavior between moderately altered volcanic zone and highly altered sheeted dike complex (Harris et al., 2008; Flynn et al., 2008). From U isotopes, ^{234}U-^{238}U disequilibria were used to determine the timing and extent of off-axis alteration at Hole 1256D (Flynn et al., 2008). While the volcanic zone was in isotopic equilibrium and indicates early alteration (i.e. close to the ridge axis), significant ^{234}U excess in the sheeted dike complex suggests later alteration (< 1.25Myr; Flynn et al., 2008). The low degree of alteration of the volcanic zone may be explained by early emplacement of a very massive lava flow, called lava pond (see depth profile in Figure 3), covering all other inflated and sheet flows. This may have set a sealing roof that would have considerably reduced the exchanges of fluids between oceanic crust and seawater, at least for the immediately underlying lavas. Moreover, fast spreading crust is smooth and rapidly buried, limiting oxidation by seawater for the 800 m thick lava sequence (Alt and Teagle, 2003; Alt et al., 2010).

The physico-chemical conditions can also be discussed from the variability of $\delta^{13}C$ with depth (Figure 3). While mean $\delta^{13}C$ value increases with depth down to the bottom of the volcanic section, the total C concentration does not show any specific trend and, on average, is constant. These two features can be explained by changes in the proportion of carbonates versus organic compounds, with an increase of carbonates associated to a decrease of organic compounds. The variation of the C_{OC}/C_{carb} ratio could result either from (1) a variation of the oxygen fugacity (fO_2), with more reducing conditions on the surface (coupled to more organic compounds) and more oxidizing conditions at depth coupled to carbonates precipitation; or (2) a variation of temperature. The first hypothesis is unlikely since progressive water-rock interaction with depth leads to more reducing fluids. Thus, we suggest that the variation of the C_{OC}/C_{carb} ratio is mostly controlled by temperature. The increase of temperature from lavas to dikes is well established qualitatively from petrological observation (this study) and quantitatively from O isotope measurements (Alt et al., 2008; Alt et al., 2010).

5.3. Microbial or abiotic synthesis of organic compounds?

An important question concerns the origin of the organic compounds detected in samples from Hole 1256D, and particularly whether they are formed through microbial or abiotic reactions. While this question may not be completely solved from the present data, part of the answer can be brought by simple observations. In basement samples from Hole 1256D, the temperature of alteration from the top of the volcanic section to bottom gabbroic rocks covers a wide range from ~50 to 950°C, respectively (Table 1; see also Alt et al., 2010). Microbial activity is known to be limited to temperature lower than ~120°C, with the upper temperature border of life organisms being represented by hyperthermophilic bacteria and archaea (e.g. Stetter, 2006). In oceanic crust, bioalteration textures are abundant mostly in a temperature range from 20°C to 80°C, and may occur up to ~110°C (Furnes and Staudigel, 1999). For samples from Hole 1256D, the temperatures of alteration (Table 1) reached more than 110°C at depth greater than 1000 mbsf, indicating that microbial activity is not expected to be sustained in deeper levels (i.e. Transition Zone, Sheeted Dike Complex and Gabbros). The organic compounds identified in the deep zones are thus produced abiotically. In contrast, for the low temperature (<110°C) zones of the section, we cannot preclude the formation of these compounds through a biological process. Notably, the $\delta^{13}C$ value of the organic endmember (~ -28‰) is compatible with typical C isotope fractionation of living organism. For instance, hydrocarbons in petroleum typically have $\delta^{13}C$ ranging from -25‰ to -35‰ (e.g. Yeh and Epstein, 1981; see Galimov, 2006 and references therein).

Because the organic compound formation seems to be abiotic, at least in the deep section of the oceanic crust, it is important to explore in detail this mechanism and test whether this hypothesis is realistic. Since the evidence of large amounts of H_2 and CH_4 in deep-sea hydrothermal fluids, the abiotic synthesis of organic compounds, such as light hydrocarbons, has been widely studied over the last decades (e.g. Charlou et al., 1998; Kelley and Früh-Green, 1999). The principle for such reactions is that hydrothermal alterations of Fe-rich rocks produces large amounts of H_2 from coupling the oxidation of Fe (II) into Fe(III) to the reduction of water into H_2. Such reaction is efficient in the case of peridotite serpentinization, where olivine reacts with water to form serpentine + brucite + magnetite. This leads the iron to be oxidized and precipitate as magnetite; while in the meantime H_2 is formed from reduction of water. Trying to quantify the H_2 production during these reactions, which is controlled by the partitioning of iron and its oxidation state during the serpentinization process, is still not an easy task. Recent detailed studies of altered peridotites (Klein et al., 2009) as well as numerical models (McCollom and Bach, 2009) have shown for example the importance of several parameters such as temperature, water-rock ratio, silica

activity in the fluid as well as rock composition. Moreover, magmatic events might also be responsible for high H_2 production such as shown by Lilley et al. (2003) at vent of the fast spreading EPR 9°N. We can conclude that in the most favorable cases, low oxygen fugacities are generated in these systems, leading to the possible reduction of CO_2 (or DIC) via a series of reactions leading to formic acid (HCOOH), CO, CH_4 and longer chain hydrocarbons. The most widely invoked mechanism, even if it is not the unique one, to interpret this abiotic synthesis of organic compounds is the Fischer-Tropsch-type (FTT) reaction which strictly speaking concerns only the formation of organic compounds from a gaseous mixture of CO and H_2. Hydrothermal alteration of more silica-rich basaltic rocks generally produces less H_2 since it produces minerals (like chlorite, amphibole) whose structures accept Fe(II) which is then less easily oxidized to Fe(III). Even if serpentinites appear to be unique in their capacity to generate high H_2 abundances, water-basalt interaction can produce moderately to strongly reducing conditions with H_2 concentrations in the range 0.05-1.7 mmol/kg (measured in deep-sea hydrothermal fluids that interacted with hot basalts; Von Damm, 1995) to be compared with 12-16 mmol/kg in ultramafic rocks (e.g. Charlou et al., 2002). Whether such H_2 concentration is high enough to induce reduction of carbon from magmatic CO_2 and produce, partly or completely, the organic compounds precipitated in our samples or not can be tested via thermodynamic and isotope composition considerations.

Shock and Schulte (1998) studied thermodynamic equilibrium involved during organic synthesis in deep-sea hydrothermal systems and showed that for temperatures below 400°C, the reaction:

$$CO_2 + 4H_2 \Leftrightarrow CH_4 + 2H_2O \quad (4)$$

is displaced to the right side, suggesting that fluids equilibrated at low temperatures are CH_4-rich. This reaction can be compared with calculated hydrogen fugacities set by the FMQ (fayalite-magnetite-quartz) and PPM (pyrite-pyrrhotite-magnetite) buffer which are the two main mineral buffers in seawater-basalt systems depending upon depth (Shock, 1990). From this comparison, it appears that for pyrrhotite-pyrite-magnetite buffered systems, CO_2 reduction into CH_4 will be efficient at T <250-300°C. Even if methane is the most thermodynamically favored stable organic compound at these conditions, kinetic barriers existing at these temperature allow the metastable synthesis of others organic compounds. This is coherent with the experimental work of Rushdi and Simoneit (2001) which shown that the maximum lipid yield during an aqueous Fischer-Tropsch-type reactions was the 150-250°C temperature window. This is in good agreement with the present observation that the C_{OC}/C_{tot} ratio in Hole 1256D samples is larger in the upper part of the volcanic section and

631 decreases with depth as temperature increases. From these observations, the following
632 scenario can be proposed. Fluid-rock interaction during heating of seawater will increase H_2
633 concentrations. As fluids approach high-temperature reaction zone in the deeper part of the
634 crust, increased reaction rates may supply additional H_2 to the system from reaction with
635 basalts while injection of CO_2-dominated magmatic gases will provide additional carbon.
636 When these CO_2- and H_2-charged high temperature fluids cool down either by conduction
637 and/or mixing with seawater during ascent to the seafloor at the spreading axis, or close to the
638 spreading axis, it induces a large thermodynamic drive for the production of organic
639 compounds through equation 4. Even if abiotic synthesis is thermodynamically favored in
640 deep-sea hydrothermal systems, there are however large kinetic barriers for these reactions to
641 occur at temperatures below 350°C (McCollom and Seewald, 2007). Numerous experimental
642 works studied the FTS reactions (for comprehensive reviews of FTS research see Anderson,
643 1984; Dry, 1981) and in particular the most suitable catalysts to enhance the reaction (e.g.
644 magnetite, metal Fe, Fe-Ni alloys, chromite). If we consider the only experiments performed
645 in aqueous solution, which are the most appropriate for interpreting natural systems, the
646 presence of a vapor phase, existing when large amounts of H_2 and CO_2 are produced, as well
647 as chromite, could be the factor that allows FTT reactions to proceed rapidly and to enhance
648 the formation of complex hydrocarbons species (McCollom and Seewald, 2007, Foustoukos
649 and Seyfried, 2004). To conclude, all the experimental works indicate that FTT reactions can
650 proceed rapidly in hydrothermal environments.
651 Another argument that can be used to discuss the origin of the newly formed organic
652 compounds is its isotopic composition, mainly $\delta^{13}C$ since no measurements of δD were done
653 in any experimental work. In their study, McCollom and Seewald (2006) measured the
654 isotope composition of each carbon compound formed during reduction of formic acid in the
655 presence of Fe powder at 250°C and 325 bar. They showed that the synthesized hydrocarbons
656 were significantly depleted in ^{13}C relative to the dissolved CO_2, with a fractionation of ~ 36
657 ‰. The present data allow us to estimate the C isotope fractionation between oxidized
658 magmatic C and organic compounds formed in altered oceanic crust. Assuming that the
659 lowest $\delta^{13}C$ value measured in our samples represents the C isotope composition of organic
660 compounds (i.e. -26.6 ‰) and that magmatic C has a $\delta^{13}C$ value around -5‰, then the
661 calculated fractionation is ~21‰. Even if there might be kinetic effects that make this reaction
662 non-equilibrium, the present data are of similar direction (i.e. hydrocarbon depletion in ^{13}C)
663 and order of magnitude than the experimental value of ~ 36 ‰. We thus conclude that, taking

664 into account all these uncertainties, the $\delta^{13}C$ values measured in samples from Hole 1256D
665 are compatible with a production of organic compounds by FT synthesis. An abiotic process
666 is necessary for the deeper part of the crust but, even if not required, we cannot rule out the
667 contribution of microbial activity at low-temperature in the shallow alteration zones.
668
669 **5.4. Implication for the global C geodynamic cycle**
670
671 In good agreement with previous studies (Staudigel et al., 1989; Alt and Teagle,
672 1999), samples from Hole 1256D illustrate that background alteration of oceanic crust
673 induces a carbon-enrichment in the rocks. Alt and Teagle (1999) showed that, with aging,
674 oceanic crust is progressively enriched in carbonates by successive steps of seawater-crust
675 alteration. In the present paper, we studied a young section of oceanic crust (~15 Ma) that
676 experienced limited seawater-rock interaction. We show that carbon in Hole 1256D mainly
677 occurs as reduced species, i.e. organic compounds. The source of this C is likely magmatic
678 CO_2 (i) degassed from the mantle at or near ridge axis, (ii) subsequently mixed with
679 hydrothermal fluids and (iii) reduced through fluid-crust interaction (see discussion above in
680 part 5.1.1).
681 Integrating the present results with previous data, we can propose the following global
682 model for C cycling during oceanic crust alteration (Figure 6). First, when oceanic crust is
683 formed at ridge axis, it experiences interaction with hydrothermal fluids enriched in magmatic
684 CO_2. These physico-chemical conditions promote the reduction of magmatic C to CH_4 and
685 other organic compounds during ascent and cooling of the fluid. While CH_4 is transferred to
686 seafloor vents by fluid flow, heavy insoluble organic compounds are trapped into the crust. It
687 is worth noting that the reduction of magmatic CO_2 into organic compounds is only partial
688 compared to the flux of degassed magmatic C since $\delta^{13}C_{oc}$ measured in our samples are ~ -25
689 ‰. In the case of total reduction, $\delta^{13}C_{oc}$ would have been similar to magmatic C (i.e. $\delta^{13}C$ ~ -
690 5‰), which is not observed. This is also in good agreement with C isotope composition of
691 CO_2 in hydrothermal fluids released in seafloor vents, which show $\delta^{13}C$ values
692 undistinguishable from magmatic CO_2 (Charlou et al., 1996; Kelley and Früh-Green, 1999)..
693 In a second step of alteration, when the crust moves away from the ridge axis, the influence of
694 the hydrothermal convection of hot fluids enriched in magmatic CO_2 rapidly decreases and
695 becomes negligible. The C input into the crust is then mainly controlled by late carbonate
696 precipitation from seawater bicarbonates mostly in the volcanic section, which remains

sufficiently permeable to support ongoing convection even in old crust. In contrast, sheeted dikes and gabbros are less permeable and not affected anymore by hydrothermal fluid convection since they are far away from the heating source (i.e. magma chamber; e.g. Alt et al., 1986, Alt et al., 1996). With aging, the volcanic section may experience successive seawater infiltrations that enhance carbonate precipitation. In this model of alteration, C contained as organic compounds would be mainly derived from outgassed mantle CO_2, while C present as carbonates would be dominantly derived from seawater (Figure 6). If this model is true, the amount of C as organic compounds added to a section of oceanic crust should not evolve from few million years-old to hundred million years. We thus anticipate that if organic carbon is measured in other drill-holes from the oceanic crust, a significant amount of organic component will be revealed. This amount will probably be independent of the age of the crust and may show values similar to those measured in Hole 1256D samples, i.e. at the level of one thousand ppm CO_2 if no biotic organic C is added over this long period of time. This will need to be confirmed in future studies on samples from other drill-holes such as DSDP/ODP 504B, ODP 896 or 801, in which the rocks are more heavily altered than in Hole 1256D.

On the basis of hundreds of bulk rock analyses combined with vein carbonate data, Alt and Teagle (1999) estimated the flux of total C (including carbonate and organic carbon) uptake during alteration of oceanic crust. While this value is quite robust considering the high amount of data and the wide variety of sites taken into consideration, no distinction was made between C components, particularly whether C occurs as carbonate or organic carbon. The present study of Hole 1256D provide an opportunity to estimate the concentrations and isotope composition of these C bearing phases. Using the global model for C cycling presented above, we can assume that the flux of total C uptake determine by Alt and Teagle (1999) is composed by carbonates and organic carbon. While carbonate content will depend on the age of the crust, organic carbon will be produced and trapped mainly close to the ridge axis if coming from magmatic CO_2. For biogenic organic carbon, there exist indirect evidences from S isotopes (Rouxel et al., 2008; Alt et al., 2003, 2007) that support long lasting microbial activity in oceanic crust. This microbial activity might contribute to add organic carbon. At the present time, the production rate of such biogenic process is not known. Thus on first order, Hole 1256D is considered as representative of the mean oceanic crust for its organic carbon content. For each main lithological unit of the altered oceanic crust, we have calculated a mean organic carbon content from the results obtained on our samples (Table 6). The mean carbonate contents were then calculated as the difference between total C content from previous estimate (Alt and Teagle, 1999) and organic C content

731 determined herein. Table 6 shows that in the upper part of the crust (volcanic section and
732 transition zone), C budget is dominated by the carbonate, while in the lower part (sheeted
733 dikes and gabbros) organic compounds are preponderant. This finding supports our model for
734 C cycling, where organic C is added close to the ridge while carbonate is mainly provided to
735 the upper crust by later alteration. For the bulk crust, the depth-weighted average C contents
736 for carbonates and organic compounds are 0.17 and 0.04 wt% CO_2 respectively, giving a total
737 carbon content at ~0.21 wt% CO_2 (Alt and Teagle, 1999). From these average concentrations
738 for carbonate and organic carbon, we can calculate $\delta^{13}C$ value of the mean altered oceanic
739 crust assuming that (i) carbonate $\delta^{13}C$ are ~0.4 ‰ (average value for carbonates occurring in
740 veins measured by Coggon et al., 2006), and (ii) organic carbon $\delta^{13}C$ is -26.6 ‰ (the most
741 negative value measured in our samples from Hole 1256). This gives a mean altered oceanic
742 crust with $\delta^{13}C$= -4.7‰, similar to the $\delta^{13}C$ of the carbon degassed from the mantle at mid-
743 ocean ridges (Mattey et al., 1984; Sakai et al.,1984; Pineau and Javoy, 1994; Pineau et al.,
744 2004; Aubaud et al., 2004). Considering a crustal production rate of $6.0\pm0.8 \times 10^{16}$ g/year
745 (Mottl, 2003) and the average total C content of Alt and Teagle (1999), the total flux of C
746 stored in altered oceanic crust is $2.9\pm0.4 \times 10^{12}$ molC/yr; part of it being due to the alteration
747 process, while another part is the initial magmatic carbon. This flux can be compared with the
748 flux of C degassed from the mantle by mid-ocean ridge (MOR) systems. The flux of C
749 degassed from the mantle has been controversial for more than 20 years and various estimates
750 range over one order of magnitude from $\sim2 \times 10^{12}$ to 2×10^{13} molC/yr (e.g. Javoy et al., 1982,
751 1983; Des Marais, 1985; Javoy and Pineau, 1991; Marty and Tolstikhin, 1998; Cartigny et al.,
752 2001; Cartigny et al., 2008). Accordingly, the flux of C uptake in the altered oceanic crust is
753 either lower (≈ 0.15) or similar (≈ 1.5) to the flux degassed from the MOR. Another important
754 question is how this flux compares to the fluxes of C buried in subduction zone by
755 sedimentary material and C outgassed from subduction-related volcanism. The amount of C
756 in sedimentary material buried in subduction zones ($\sim8.9 \times 10^{11}$ molC/yr; Plank and
757 Langmuir, 1998) is 3 times lower than the C flux transferred by subducting altered oceanic
758 crust ($2.9\pm0.4 \times 10^{12}$ molC/yr; Alt and Teagle, 1999; this study). Thus, the altered oceanic
759 crust is the main carrier of C within the subducting slab. This illustrates again the importance
760 to determine precisely in future studies C concentration and isotopic composition of the bulk
761 altered oceanic crust. Including sediments and altered oceanic crust, the total flux of C buried
762 in the subducting oceanic lithosphere ($\sim3.8 \times 10^{12}$ molC/yr) is more than twice higher than the
763 flux of C outgassed from volcanic arc in subduction zones ($\sim1.6 \times 10^{12}$ molC/yr; Hilton et al.,

764 2002). This suggests that more than 50% of the C buried in subduction zones may be recycled
765 to the deep mantle and not transferred back to the surface via arc volcanism. This conclusion
766 is in good agreement with thermodynamic calculation on the stability of C-bearing phases in
767 various subducting lithologies, i.e. metasediments and metabasalts, showing that C is very
768 stable in the solid phases (i.e. carbonate and graphite) under pressure-temperature conditions
769 representative of subduction environments (e.g. Kerrick and Connolly, 2001a, 2001b). The
770 only way to induce decarbonation is by leaching of the rock through large flux of fluid
771 infiltration (Kerrick and Connolly, 2001a, 2001b). It can be noted that such a conclusion is
772 also supported from experiments under high-pressure (HP) to ultra-high pressure (UHP)
773 experiments (Poli et al., 2009). An important remaining question is whether part of the
774 subducting C is lost in early stages of subduction zone before reaching the depth locus of
775 island arc magmatism (i.e. 90-100 km). Studies of metamorphic rocks in paleo-subduction
776 zones show that volatile elements can be strongly affected by metamorphic devolatilization
777 when the rock experiences high-temperature metamorphism (e.g. Bebout, 1995). However,
778 the study of metamorphic suites subducted along "cool" geothermal gradient (8°C/km),
779 typical of present day peripacific subduction zone environment, show that volatile and fluid-
780 mobile elements can be preserved down to >90km depth (Busigny et al., 2003). Accordingly,
781 current subduction of altered oceanic crust may represent a way for natural transfer of huge C
782 amount from the surface to the deep mantle.
783
784
785 **6. CONCLUSION**
786
787 In the present contribution, C and H abundances as well as $\delta^{13}C$ and δD values are
788 reported for 19 samples of 15Ma oceanic crust cored at ODP/IODP Hole 1256D (Leg 206,
789 Expeditions 309 and 312). Hole 1256D is quite unique since it is the first hole drilled through
790 lavas, sheeted dike complex and gabbros, thus representing the most complete section of
791 oceanic crust ever sampled. While the present samples correspond to background alteration
792 (i.e. neither veins nor alteration halos adjacent to veins), significant enrichments of C and H
793 relative to fresh basalts are observed. Hydrogen isotopes are interpreted as a mixing between
794 primary magmatic hydrogen and a secondary source that can be secondary hydrous minerals
795 and/or hydrogen from organic molecules such as hydrocarbon. Carbon isotopes are
796 interpreted as a mixing between organic compounds with $\delta^{13}C \sim -27‰$, and carbonates with
797 $\delta^{13}C \sim 0‰$. The light C isotope signature of the present samples (average ~ -22 ± 2‰, 1σ)

points to a dominant contribution of the organic compounds relative to carbonates. This finding is also supported by independent measurement of carbonate abundances. Considerations about C concentrations in various geological components (i.e. fresh and altered rocks, DIC and DOC in seawater, hydrothermal fluids) drive us to the conclusion that magmatic CO_2 added to hydrothermal fluids is the main source of C ultimately transferred to the altered oceanic crust while seawater DIC and DOC represent only a minor source of C. Since C in samples from Hole 1256D mainly occurs as reduced organic compounds, a CO_2 origin implies a reduction step during alteration that can be either biologically mediated or not. If the making of this reduced organic compounds is restricted to the vicinity of the ridge where magmatic CO_2-rich and low oxygen fugacity (H_2-rich) fluids are flushed through the oceanic crust, it is likely that during the aging of the oceanic crust the dominance of reduced organic compounds decrease to the profit of carbonates which gets progressively more concentrated due to seawater inputs at the top of the oceanic crust (Staudigel et al., 1981; Alt and Teagle 1999). Analysis of other young and older oceanic crust sections for both reduced and carbonate carbon are needed to test this proposal.

ACKNOWLEDGMENTS

We thank the Institut de Physique du Globe de Paris which supported the visit of Dr. Svetlana Shilobreeva to the laboratory of stable isotope geochemistry. Dr. Shilobreeeva also benefited from grants of the CO_2 IPGP-Total-Schlumberger-ADEME Research Program, as well as grants from ANR CO2FiX. This research was made possible by samples and data provided by the Integrated Ocean Drilling Program (IODP). We are grateful to Christelle Roudaut for help in isotope measurements, to Jean-Jacques Bourrand and Guillaume Landais for their technical assistance. Helpful discussions with Françoise Pineau, Cyril Aubaud and Marc Javoy were greatly appreciated. We greatly thank Wolfgang Bach and Adélie Delacour for their constructive reviews. Jeff Alt is particularly acknowledged for handling and reviewing carefully the manuscript. This is an IPGP contribution N° 3094.

REFERENCES

Agrinier P., Laverne C. and Tartarotti P. (1995a) Stable isotope ratios (oxygen, hydrogen) and petrology of hydrothermally altered dolerites at the bottom of the sheeted dike complex of Hole 504B. *Proc. Ocean Drill. Program Sci. Results* **137**, 99-106.

833 Agrinier P., Hekinian R., Bideau D. and Javoy M. (1995b) O and H stable isotope
834 compositions of oceanic crust and upper mantle rocks exposed in the Hess Deep near the
835 Galapagos Triple Junction. *Earth Planet. Sci. Lett.* **136**, 183-196.

836 Alt J.C. (1995) Subseafloor processes in mid-ocean ridge hydrothermal systems. In *Seafloor*
837 *hydrothermal Systems: Physical, Chemical, and Biological Interactions* (Eds. Humphris, S.,
838 Lupton, J., Mullineaux, L., Zierenberg, R.) Geophysical Monograph 91, AGU, Washington
839 DC, pp. 85-114.

840 Alt, J.C. (2003) Stable isotopic composition of upper oceanic crust formed at fast speading
841 ridge, ODP Site 801. *Geochem. Geophys. Geosyst.* **4**, 8908, DOI:10.1029/2002GC000400.

842 Alt J. C., Honnorez J., Laverne C. and Emmermann R. (1986) Hydrothermal alteration of a 1
843 km section through the upper oceanic crust, deep sea drilling project hole 504B: mineralogy,
844 chemistry and evolution of seawater-basalt interactions. *J. Geophys. Res.* **91**, 10309-10335.

845 Alt J.C., Laverne C., Vanko D., Tartarotti P., Teagle D.A.H., Bach W., Zuleger E., Erzinger
846 J., Honnorez J., Pezard P.A., Becker K., Salisbury M.H. and Wilkens, R.H. (1996)
847 Hydrothermal alteration of a section of upper oceanic crust in the eastern equatorial Pacific :
848 A synthesis of results from Site 504 (DSDP legs 69, 70 and 83, and ODP legs 111, 137, 140,
849 and 148). In *Proc. Ocean Drill. Prog. Sci. Results* (Eds. Alt, J.C., Kinoshita, H., Stokking,
850 L.B., Michael, P.J.), Ocean Drilling Program, 148, pp. 417-434.

851 Alt J. C. and Teagle D.A.H. (1999) The uptake of carbon during alteration of ocean crust.
852 *Geochim. Cosmochim. Acta* **63**, 1527-1535.

853 Alt J. C. and Teagle D.A.H. (2003) Hydrothermal alteration of upper oceanic crust formed at
854 fast-spreading ridge: mineral, chemical, and isotopic evidence from ODP Site 801. *Chem.*
855 *Geol.* **201**, 191-211.

856 Alt, J.C., Davidson, G.J., Teagle, D.A.H., Karson, J.A. (2003) Isotopic composition of
857 gypsum in the Macquarie Island ophiolite: Implications for the sulfur cycle and the subsurface
858 biosphere in oceanic crust. *Geology* 31, 549-552.

859 Alt J. C. and Laverne C. (2006) Data report: Chemical compositions of secondary minerals
860 from Site 1256 basement, ODP Leg 206. In *Proc. ODP, Sci. Results,* 206 (Eds. Teagle
861 D.A.H., Wilson D.A., Acton G.A., Vanko D.A.). Available online from http://www-
862 odp.tamu.edu/publications/206_SR/003/003.htm.

863 Alt, J.C., Shanks III, W.C., Bach, W., Paulick, H., Garrido, C.J., Beaudoin, G. (2007)
864 Hydrothermal alteration and microbial sulfate reduction in peridotite and gabbro exposed by
865 detachment faulting at the Mid-Atlantic Ridge, 15°20'N (ODP Leg 209): A sulfur and oxygen
866 isotope study. *Geochemistry Geophysics Geosystems* 8, Q08002,
867 doi:10.1029/2007GC001617.

868 Alt J. C., Coggon R., Laverne C., Smith-Duque C. Teagle D. A., Morgan S. (2008) The
869 thermal structure of a submarine hydrothermal system, ODP/IODP Hole 1256D. *Eos Trans.*
870 *AGU*, **89**(53), Fall Meet. Suppl., Abstract V44B-06.
871
872 Alt J.C., Laverne C., Coggon R., Teagle D.A.H., Morgan S., Smith-Duque C., Banerjee N.R.,
873 Galli L. (2010) The subsurface structure of a submarine hydrothermal system in ocean crust
874 formed at the East Pacific Rise, ODP/IODP Site 1256. Submitted to *Geochemistry*
875 *Geophysics Geosystems*.

876 Anderson R.B. (1984) The Fischer-Tropsch reaction. Academic Press, London.
877

878 Aubaud C., Pineau F., Jambon A., Javoy M. (2004) Kinetic disequilibrium of C, He, Ar and
879 carbon isotopes during degassing of mid-ocean ridge basalts. *Earth Planet. Sci. Lett.* **222**,
880 391-406.

881 Bach W.S, Alt J.C., Niu Y., Humphris S.E., Erzinger J. and Dick H.J.B. (2001) The
882 geochemical concequences of late-stage low-grade alteration of lower ocean crust at the SW
883 Indian Ridge: Results from ODP Hole 735B (leg 176). *Geochim. Cosmochim. Acta* **65**, 3267-
884 3287.

885 Bach W., Bernhard P-E., Hart S. and Blusztajn J.S. (2003) Geochemistry of hydrothermally
886 altered crust: DSDP/ODP Hole 504B – implications for seawater-crust exchange budgets and
887 Sr- and Pb-isotopic evolution of the mantle. *Geochemistry Geophysics Geosystems* **4,**
888 doi:10.1029/20002GC000419.

889 Banerjee N.R. and Honnorez J. (2004) Data report: Low-temperature alteration of upper
890 oceanic crust from the Ontong Java Plateau, Leg 192: alteration and vein logs. In *Proc. ODP,*
891 *Sci. Results*, **192** (Eds. Fitton, J.G., Mahoney J.J., Wallace P.J., and Saunders A.D.),
892 http://www-odp.tamu.edu/publications/192_SR/103/103.htm.

893 Bauer J.E., Druffel E.R.M., Wolgast D.M., Griffin S. and Masiello C.A. (1998), Distributions
894 of dissolved organic and inorganic carbon and radiocarbon in the eastern North Pacific
895 continental margin. *Deep-sea Research Part II-Topical studies in oceanography* **45**, 4-5, 689-
896 713.

897 Bebout G.E. (1995) The impact of subduction-zone metamorphism on mantle-ocean chemical
898 cycling. *Chem. Geol.* **126**, 191-218.

899 Bottinga Y. (1969) Carbon isotope fractionation between graphite, diamond and carbon
900 dioxide. *Earth Planet. Sci. Lett.* **5**, 301-306.

901 Busigny V., Cartigny P., Philippot P., Ader M. and Javoy M. (2003) Massive recycling of
902 nitrogen and other fluid-mobile elements (K, Rb, Cs, H) in a cold slab environment:
903 Evidences from HP to UHP oceanic metasediments of the Schistes Lustrés nappe (Western
904 Alps, Europe). *Earth and Planet. Sci. Lett.* **215**, 27-42.

905 Busigny V., Laverne C. and Bonifacie M. (2005) Nitrogen content and isotopic composition
906 of ocean crust at a superfast spreading ridge: A profile in altered basalts from ODP Site 1256,
907 Leg 206. *Geochemistry Geophysics Geosystems* **6**, Q12O01, doi:10.1029/2005GC001020.

908 Capuano R.M. (1992) The temperature dependence of hydrogen isotope fractionation between
909 clay minerals and water: Evidence from a geopressured system. *Geochim. Cosmochim. Acta*
910 **56**, 2547-2554.

911 Cartigny P., Jendrzejewski N., Pineau F., Petit E. and Javoy M. (2001) Volatile (C, N, Ar)
912 variability in MORB and the respective roles of mantle source heterogeneity and degassing:
913 the case of the Southwest Indian Ridge. *Earth Planet. Sci. Lett.* **194,** 241-257.

914 Cartigny P., Pineau F., Aubaud C. and Javoy M. (2008) Towards a consistent mantle carbon
915 flux estimate: insights from volatile systematics (H_2O/Ce, δD , CO_2/Nb) in the North Atlantic
916 mantle (14°N and 34°N). *Earth Planet. Sci. Lett.* **265**, 672-685.

917 Chacko T., Cole D.R., and Horita J. (2001) Equilibrium oxygen, hydrogen and carbon isotope
918 fractionation factors applicable to geological systems. In *Stable Isotope Geochemistry* (Eds
919 J.W. Valley and D. R. Cole), Reviews in Mineralogy and Geochemistry 43. Washington DC,
920 pp 1–81.

921 Charlou J.L., Fouquet Y., Donval J.P., Auzende J.M., Jean-Baptiste P., Stievenard M. and
922 Michel S. (1996) Mineral and gas chemistry of hydrothermal fluids on an ultrafast speading
923 ridge: East Pacific Rise, 17° to 19°S (Naudur cruise, 1993) phase separation processes
924 controlled by volcanic and tectonic activity. *J. Geophys. Res.* **101**, 15899-15919.

925 Charlou J.L., Fouquet Y., Bougault H., et al. (1998) Intense CH_4 plumes generated by
926 serpentinization of ultramafic rocks at the intersection of the 12°20'N fracture zone and the
927 Mid-Atlantic Ridge. *Geochim. Cosmochim. Acta* **62**, 2323-2333.

928 Charlou J.L., Donval J.P., Douville E., Jean-Baptiste P., Radford-Knoery J., Fouquet Y.,
929 Dapoigny A. and Stievenard M. (2000) Compared geochemical signatures and the evolution
930 of Menez Gwen (37°50'N) and Lucky Strike (37°17'N) hydrothermal fluids, south of the
931 Azores Triple Junction on the Mid-Atlantic Ridge. *Chem. Geol.* **171**, 49-75.

932 Charlou J.L., Donval J.P., Fouquet Y., Jean-Baptiste P. and Holm N. (2002) Geochemistry of
933 high H2 and CH4 vent fluids issuing from ultramafic rocks at the Rainbow hydrothermal field
934 (36°14'N, MAR). *Chem. Geol.* **191**, 345-359.

935 Coggon R.M., Teagle D.A.H., Cooper M.J., Hayes T.E.F. and Green D.R.H. (2006) Data
936 report: Compositions of Calcium Carbonate Veins from Superfast Spreading Rate Crust, ODP
937 Leg 206. *Proceedings of the Ocean Drilling Program, Scientific Results* **206**, 1-6.
938
939 Craig H. and Lupton J.E. (1976) Primordial neon, helium, and hydrogen in oceanic crust.
940 *Earth Planet. Sci. Lett.* **31**, 369–385.

941 Delacour A., Früh-Green G.L., Bernasconi S.M., Schaeffer P. and Kelley D.S. (2008) Carbon
942 geochemistry of serpentinites in the Lost City Hydrothermal System (30°N, MAR). *Geochim.*
943 *Cosmochim. Acta* **72**, 3681–3702.

944 Des Marais D.J. (1985) Carbon exchange between the mantle and the crust, and its effect
945 upon the atmosphere : today compared to Archean time. In *The carbon cycle and atmospheric*
946 *CO2: natural variations from Archean to present* (Eds. E.T. Sundquist, W.S. Broecker), AGU
947 Geophysical Monograph. 32, pp. 602-611.

948 Des Marais D.J., Strauss H., Summons R.E. and Hayes J.M. (1992) Carbon isotope evidence
949 from the stepwise oxidation of the proterozoic environment. *Nature* **359**, 605-609.

950 Dry M.E. (1981) The Fischer-Tropsch Synthesis. In *Catalysis: Science and Technology* (Eds.
951 Anderson J.R., Boudart, M.), Springer Verlag, New York, pp. 159-255.

952 Flynn K.S., Cooper K.M., Teagle D.A., Banerjee N., Smith-Duque C.E., Harris M., Coggon
953 R.M. and Cooper M. (2008) Timing of alteration from uranium-series geochemistry of altered
954 ocean crust at IODP Site 1256D. *Eos Trans. AGU*, **89**(53), Fall Meet. Suppl., Abstract V51F-
955 2098.

956 Foustoukos D.I. and Seyfried W. (2004) Hydrocarbons in hydrothermal vent fluids: the role
957 of chromium-bearing catalysts. Science, **304**, 1002-1005.

958 France L., Ildefonse B. and Koepke J. (2009) Interactions between magma and hydrothermal
959 system in Oman ophiolite and in IODP Hole 1256D: Fossilization of a dynamic melt lens at
960 fast spreading ridges. *Geochemistry Geophysics Geosystems* **10**, Q10O19,
961 doi:10.1029/2009GC002652.

962 Friedrichsen H. and Hoernes S. (1979) Oxygen and hydrogen isotope exchange reactions
963 between seawater and oceanic basalts from Legs 51 through 53. *Init. Rep. Deep Sea Drill.*
964 *Proj.* **51-53**, 1177-1182.
965

966 Friedrichsen H. (1985) Strontium, oxygen and hydrogen isotope studies on primary and
967 secondary minerals in basalts from the Costa Rica Rift, Hole 504B, Leg 83. *Init. Rep. Deep*
968 *Sea Drill. Proj.* **83**, 289-296.

969 Furnes H. and Staudigel H. (1999) Biological mediation in ocean crust alteration: how deep is
970 the deep biosphere? *Earth Planet. Sci. Lett.* **166,** 97-103.

971 Furnes H., Muehlebachs K., Torsvik T., Thorseth I.H. and Tumyr O. (2001) Microbial
972 fractionation of carbon isotopes in altered basaltic glass from the Atlantc Ocean, Lau Basin
973 and Costa Rica Rift. *Chem. Geol.* **173**, 313-330.

974 Galimov E. (2006) Isotope organic geochemistry. *Organic Geochemistry* 37, 1200-1262.

975 Graham C.M., Harmon R.S. and Sheppard S.M.F (1984) Experimental hydrogen isotope
976 studies: hydrogen isotope exchange between amphibole and water. *Amer. Mineral.* **69**, 128-
977 13.

978 Graham C.M., Viglino J.A. and Harmon R.S. (1987) Experimental study of hydrogen-isotope
979 exchange between aluminous chlorite and water and of hydrogen diffusion in chlorite. *Amer.*
980 *Mineral.* **72**, 566-579.

981 Gregory R.T. and Taylor Jr. H.P. (1981) An oxygen isotope profile in a section of Cretaceous
982 oceanic crust, Samail ophiolite, Oman: evidence for $\delta^{18}O$-buffering of the oceans by deep (>5
983 km) seawater–hydrothermal circulation at mid-ocean ridges. *Jr Geophy. Res.* **86**, 2737–2755.

984 Hansell D. A. and Carlson C. A. (1998) Deep-ocean gradients in the concentration of
985 dissolved organic carbon. *Nature* **395**, 263–266.

986 Harris M., Smith-Duque C.E., Teagle D.A., Cooper K.M., Coggon R.M. and Foley L. (2008)
987 A whole rock strontium isotopic profile through an intact section of upper oceanic crust: ODP
988 Site 1256. *Eos Trans. AGU* **89**(53), Fall Meet. Suppl., Abstract V44B-07.

989 Hilton D.R., Fischer T.P. and Marty B. (2002) Noble gases and volatile recycling at
990 subduction zones. In *Noble gases in geochemistry and cosmochemistry* (Eds. D. Porcelli, C.J.
991 Ballentine, R. Wieler), Reviews in Mineralogy and Geochemistry 47, Washington DC, pp.
992 319-370.

993 Hoernes, S. and Friedrichsen, H. (1978) $^{18}O/^{16}O$ and D/H investigations on basalts of Leg 46.
994 *Init. Rep. Deep Sea Drill. Proj.* **46**, 253-255.

995 Hyeong K. and Capuano R.M. (2004) Hydrogen isotope fractionation factor for mixed-layer
996 illite/smectite at 60° to 150°C: New data from the northeast Texas Gulf Coast. *Geochim.*
997 *Cosmochim. Acta* **68**, 1529-1543.

998 Javoy M. (1998) The birth of the Earth's atmosphere: the behaviour and fate its major
999 elements. *Chem. Geol.* **147**, 11-25.

1000 Javoy, M. and Fouillac, A.M. (1979) Stable isotope ratios in Deep Sea Drilling Project Leg 51
1001 basalts. *Init. Rep. Deep Sea Drill. Proj.* **51-53**, 1153-1157.

1002 Javoy M., Pineau F. and Allègre, C. (1982) The carbon geodynamic cycle. *Nature* **300**, 171-
1003 173.

1004 Javoy M., Pineau F. and Allègre, C. (1983) Reply - The carbon geodynamic cycle. *Nature*
1005 **303**, 731.

1006 Javoy M. and Pineau F. (1991) The volatile record of a "popping" rock from the Mid-Atlantic
1007 Ridge at 14oN: chemical and isotopic composition of gas trapped in the vesicles. *Earth*
1008 *Planet. Sci. Lett.* **107**, 598-611.

1009 Kawahata H., Kusakabe M. and Kikuchi Y. (1987) Strontium, oxygen and hydrogen isotope
1010 geochemistry of hydrothermally altered and weathered rocks in DSDP Hole 504B, Costa Rica
1011 Rift. *Earth Planet. Sci. Lett.* **85**, 343-355.

1012 Kelley D.S. and Früh-Green G.L. (1999) Abiogenic methane in deep-seated mid-ocean ridge
1013 environments: Insights from stable isotope analyses. *J. Geophys. Res.* **104**, 10439-10460.

1014 Kelley D.S. and Früh-Green G.L. (2001) Volatile lines of descent in submarine plutonic
1015 environments: Insights from stable isotope and fluid inclusion analyses. *Geochim.*
1016 *Cosmochim. Acta* **65**, 3325-3346.

1017 Kerrick D.M. and Connolly J.A.D. (2001a) Metamorphic devolatilization of subducted
1018 marine sediments and the transport of volatiles into the Earth's mantle. *Nature* **411,** 293-296

1019 Kerrick D.M. and Connolly J.A.D. (2001b) Metamorphic Devolatilization of Subducted Mid-
1020 Ocean Ridge Metabasalts: Implications for Seismicity, Arc Magmatism and Volatile
1021 Recycling. *Earth Planet. Sci. Lett.* **189**, 19-29.

1022 Klein F., Bach W., Jöns N., McCollom T., Moskowitz B. and Berquo T., (2009) Iron
1023 partitioning and hydrogen generation during serpentinization of abyssal peridotites from 15°N
1024 on the Mid-Atlantic Ridge. *Geochim. Cosmochim. Acta* **73**, 6868-6893.

1025 Koepke J., Christie D.M., Dziony W., Holtz F., Lattard D., Maclennan J., Park S., Scheibner
1026 B., Yamasaki T., Yamazaki S. (2008) Petrography of the dike-gabbro transition at IODP Site
1027 1256 (equatorial Pacific): The evolution of the granoblastic dikes. *Geochemistry Geophysics*
1028 *Geosystems* **9**, Q07O09, doi:10.1029/2008GC001939

1029 Kyser T.K. and O'Neil J.R. (1984) Hydrogen isotope systematics of submarine basalts.
1030 *Geochim. Cosmochim. Acta* **48**, 2123-2133.

1031 Laverne C., Grauby O., Alt J. C. and Bohn M. (2006) Hydroschorlomite in altered basalts
1032 from Hole 1256D, ODP Leg 206: The transition from low-temperature to hydrothermal
1033 alteration. *Geochemistry Geophysics Geosystems* **7**, Q10O03, doi:10.1029/2005GC001180

1034 Li L., Bebout G.E. and Idleman B.D. (2007) Nitrogen concentration and $\delta^{15}N$ of altered
1035 oceanic crust obtained on ODP Legs 129 and 185: Insights into alteration-related nitrogen
1036 enrichment and the nitrogen subduction budget. *Geochim. Cosmochim. Acta* **71**, 2344-2360.

1037 Libera J. and Gogotski Y. (2001) Hydrothermal synthesis of graphite using Ni catalyst.
1038 *Carbon* **39**, 1307-1318.

1039 Lilley M.D., Butterfield D.A., Lupton J.E. and Olson E.J., (2003) Magmatic events can
1040 produce rapid changes in hydrothermal vent chemistry. Nature **422**, 878-881.

1041 Marty B. and Tolstikhin I.N. (1998) CO_2 fluxes from mid-ocean ridges, arcs and plumes.
1042 *Chem. Geol.* **145**, 233-248.

1043 Marty, B. and Zimmermann, L., 1999. Volatiles (He, C, N, Ar) in mid-ocean ridge basalts:
1044 Assesment of shallow-level fractionation and characterization of source composition.
1045 *Geochim. Cosmochim. Acta* **63**, 3619-3633.
1046
1047 Mattey D.P., Carr R.H., Wright I.P., Pillinger C.T. (1984) Carbon isotopes in submarine
1048 basalts. *Earth Planet. Sci. Lett.* **70,** 196-206.

1049 McCollom T. and Seewald J.S. (2006) Carbon isotope composition of organic compounds
1050 produced by abiotic synthesis under hydrothermal conditions. *Earth Planet. Sci. Lett.* **243**, 74-
1051 84.

McCollom T. and Seewald J.S. (2007) Abiotic synthesis of organic compounds in deep-sea hydrothermal environments. *Chem. Rev.* **107**, 382-401.

McCollom T. and Bach W. (2009) Thermodynamic constraints on hydrogen generation during serpentinization of ultramafic rocks *Geochim. Cosmochim. Acta* **73**, 856-875.

McCulloch M.T., Gregory R.T., Wasserburg G.J., Talor H.P. (1981) Sm-Nd, Rb-Sr, and O-18-O-16 isotopic systematics in an oceanic crustal section-evidence from the Samail ophiolite. *J. Geophys. Res.* **86**, NB4, 2721-2735.

McCrea J.M. (1950) On the isotopic chemistry of carbonates and a paleotemperature scale. *J. Chem. Phys.* **18**, 849-857.

Mottl M.J. (2003) Partitioning of energy and mass fluxes between mid-ocean ridge axes at high and low temperature. In *Energy and Mass Transfer in Marine Hydrothermal Systems* (Eds. Halbach P.E. et al.), Dahlem University Press, pp. 271–286.

Muehlenbachs K. (1986) Alteration of the oceanic crust and ^{18}O history of seawater. In *Stable Isotopes in high temperature geological processes* (Eds. Valley J.W., Taylor H.P. Jr., O'Neil J.R.), Reviews in Mineralogy 16, Washington DC, pp 425-444.

Pineau F. and Javoy M. (1994) Strong degassing at ridge crest / the behaviour of dissolved carbon and water in basalt glasses at 14°N Mid-Atlantic Ridge. *Earth Planet. Sci. Lett.* **123**, 179-198.

Pineau F., Shilobreeva S, Hekinian R., Bideau D. and Javoy M. (2004) Deep-sea explosive activity on the Mid-Atlantic Ridge near 34°50'N: a stable isotope (C, H, O) study. *Chem. Geol.* **211**, 159-175.

Plank T. and Langmuir C.H. (1998) The chemical composition of subducting sediment: implications for the crust and mantle. *Chem. Geol.* **145**, 325–394.

Poli S., Franzolin E., Fumagalli P. and Crottini A. (2009) The transport of carbon and hydrogen in subducted oceanic crust: An experimental study to 5 GPa. *Earth Planet. Sci. Lett.* **278**, 350-360.

Proskurowski, G., Lilley, M.D., Olson, E.J. (2008) Stable isotopic evidence in support of active microbial methane cycling in low-temperature diffuse flow vents at 9°50'N East Pacific Rise. *Geochim. Cosmochim. Acta* **72**, 2005-2023.

Ravizza G., Blusztajn J., Von Damm K.L., Bra, A.M., Bach, W., Hart, S.R. (2001) Sr isotope variations in vent fluids from 9°46'-9°54'N East Pacific Rise: Evidence of a non-zero-Mg fluid component. *Geochim. Cosmochim. Acta* **65**, 729-739.

Rhusdi A.I. and Simoneit B.T. (2001) Lipid formation by aqueous Fischer-Tropsch-type synthesis over a temperature range of 100 to 400°C. *Origins of life and evolution of the biosphere* **31**, 103-118.

Rouxel O., Ono SH., Alt J., Rumble D. and Ludden J. (2008) Sulfur isotope evidence for microbial sulfate reduction in altered oceanic basalts at ODP Site 801. *Earth Planet Sci. Lett.* **268**, 110-123.

Sakai H., Des Marais D.J., Ueda A. ,Moore J.G. (1984) Concentrations and isotope ratios of carbon, nitrogen and sulfur in ocean-floor basalts**.** *Geochim.Cosmochim. Acta* **48,** 2433-2441.

Shanks W.C. III, Böhlke J.K. and Seal R.R.II (1995) Stable isotopes in mid-ocean ridge hydrothermal systems: interactions between fluids, minerals and organisms. In *Seafloor Hydrothermal Systems: Physical, Chemical, Biological, and Geological Interactions* (Eds. Humphris, S., Lupton, J., Mullineaux, L., Zierenberg, R.), Geophysical Monograph 91, AGU,

Washington DC, pp 194-221.

Shipboard Scientific Party (2003) Site 1256. In Wilson, D.S., Teagle, D.A.H., Acton, G.D., *Proc. ODP, Init. Repts., 206: College Station, TX (Ocean Drilling Program).* doi:10.2973/odp.proc.ir.206.103.2003.

Shock L.E. (1990) Geochemical constraints onthe origin of organic compounds in hydrothermal systems. *Origins of Life and Evolution of the Biosphere* **20**, 331-367.

Shock L.E., Schulte MD. (1998) Organic synthesis during fluid mixing in hydrothermal systems. *J. Geophys. Res.* **103**, 28513-28527.

Staudigel H., Hart S.R., Richardson, S.H. (1981) Alteration of the oceanic crust: processes and timing. *Earth Planet. Sci. Lett.* **52**, 311-327.

Staudigel H., Hart S.R., Schmincke H.U. and Smith B.M. (1989) Cretaceous ocean crust at DSDP sites 417 and 418: Carbon uptake from weathering versus loss by magmatic outgassing. *Geochim. Cosmochim. Acta* **53**, 3091 – 3094.

Staudigel H. (2007) Hydrothermal alteration processes in the oceanic crust. In *Treatise on geochemistry vol. 3* (Eds. H.D. Holland and K.K. Turekian), Elsevier, Amsterdam, pp. 511-535.

Stetter K.O. (2006) Hyperthermophiles in the history of life. Philosophical Transactions of the royal Society B-Biological Sciences **361,** 1474, 1837-1842.

Stichler, W. (1995) Interlaboratory comparison of new materials for carbon and oxygen isotope ratio measurements. In *Reference and intercomparison materials for stable isotopes of light elements* (Eds. International Atomic Energy Agency), IAEA-TECDOC-825, Vienna, pp. 67-74.

Taylor H.P. (1978) Oxygen and hydrogen isotope studies of plutonic granitic rocks. *Earth Planet. Sci. Lett.* **38**, 177-210.

Teagle DA.H., Alt J.C., Chiba H., Humphris S.E. and Halliday A.N. (1998) Strontium and oxygen isotopic constraints on fluid mixing, alteration and mineralization in the TAG hydrothermal deposit. *Chem. Geol.* **149**, 1-24.

Teagle D.A.H., Alt J.C., Umino S., Miyashita S., Banerjee N.R., Wilson D.S. and the Expedition 309/312 Scientists (2006) Superfast spreading rate crust 2 and 2. *Proc. Integrated Ocean Drill. Program, 309/312*, 50 pp., doi:10.2204/iodp.proc.309312.2006. (Available at http://publications.iodp.org/scientific_prospectus/309_312/index.html).

Tingle T.N., Mathez E.A., Hochella M.F. (1991) Carbonaceaous matter in peridotites and basalts studied by XPS, SALI and LEED. *Geochim. Cosmochim. Acta* **55**, 1345 – 1352.

Umino S., Lipman P.W. and Obata S. (2000) Subaqueous lava flow lobes, observed on ROV KAIKO dives off Hawaii. *Geology* **28**, 503-506.

Valley J.W. (1986) Stable isotope geochemistry of metamorphic rocks. In *Stable Isotopes in high temperature geological processes* (Eds. Valley J.W., Taylor H.P. Jr., O'Neil J.R.), Reviews in Mineralogy 16, Washington DC, pp 445-489.

Vanko D.A. (1988) Temperature, pressure, and composition of hydrothermal fluids, with their bearing on the magnitude of tectonic uplift at mid-ocean ridges, inferred from fluid inclusions in oceanic layer-3 rocks. *J. Geophys. Res.* **93,** 4595-4611.

Von Damm K.L. (1995) Controls on the chemistry and temporal variability of seafloor hydrothermal fluids. In *Seafloor hydrothermal systems: Physical, Chemical, Biological, and*

Geological interactions (Eds. Humphris S.E., Zierenberg R.A., Mullineaux I.S. and Tompson R.), Washington D.C., American Geophysical Union, Monograph, **91**, pp. 222-247.

Welhan J.A. and Lupton J.E. (1987) Light hydrocarbon gases in Guaymas Basin hydrothermal fluids: thermogenic versus abiogenic origin. *Amer. Assoc. Petrol. Geol. Bull.* **71**, 215-223.

Wilson D.S., Teagle, D.A.H., Alt J.C., Banerjee N.R., Umino S. et al. (2006) Drilling to gabbro in intact ocean crust. Drilling to gabbro in intact ocean crust. *Science* **312**, 1016-1020.

Wilson D.S. (1996) Fastest known spreading on the Miocene Cocos-Pacific plate boundary. *Geophys. Res. Lett.* **23**, 3003-3006.

Yeh H-W and Epstein S. (1981) Hydrogen and carbon isotopes of petroleum and related organic matter. *Geochim. Cosmochim. Acta*. **45,** 753-762.

FIGURE CAPTIONS

Fig. 1. Bathymetric map showing the location of ODP/IODP Hole 1256D in the Cocos Plate (modified after Shipboard Scientific Party, 2003). Location of DSDP/ODP Hole 504B is reported for comparison.

Fig. 2. Spectrum of CO_2 released by step-heating experiments for samples analyzed in this study. The various colour bands represent different conditions of extraction (250°C with O_2 pressure, 900°C without O_2, 1170°C without O_2 and 1170°C with O_2). It shows that, for all samples, most of the CO_2 is released in the step at 900°C without O_2 pressure.

Fig. 3. Depth profiles of water (a) and CO_2 (c) contents, and hydrogen (b) and carbon (d) isotope compositions in samples from Hole 1256D. Sample numbers reported in Fig. 3c are taken from Table 3, and correspond to the core-section in Tables 1 and 2.

Fig. 4. Carbon isotope composition vs CO_2 content in altered basalts from Hole 1256D. Fresh basalt glasses from Atlantic and Pacific mid oceanic ridges are represented for comparison (data from Mattey et al., 1984; Sakai et al.,1984; Pineau and Javoy, 1994; Pineau et al., 2004; Aubaud et al., 2004), as well as serpentinites from Lost City Hydrothermal System, MAR (Delacour et al., 2008).

Fig. 5. Hydrogen isotope composition vs H_2O content in altered basalts from Hole 1256D in comparison with fresh basalt glasses from Atlantic and Pacific mid oceanic ridges (data from Craig and Lupton, 1976; Kyser and O'Neil, 1984; Pineau et al., 2004), as well as altered oceanic rocks from Hess Deep, EPR (Agrinier et al., 1995b).

Fig. 6. Model of alteration based on C isotopic composition. A two-step model is proposed: (a) close to ridge axis where hot CO_2-rich hydrothermal fluids interact with rocks, promoting reducing conditions and CH_4 and other organic compounds production. This reaction is attested by the very negative $\delta^{13}C$ values (~ -26‰) measured in our samples. (b) when crust moves away from ridge axis, the influence of these hot fluids becomes negligible. Carbon is incorporated into the crust only through seawater infiltration and carbonate precipitation, forming veins in the upper part of the volcanic section.

Table 1. Petrological, mineralogical and alteration features of samples from this study (ODP/IODP Hole 1256D).

Core-section, Interval (cm)	Depth (mbsf)	Spl #	Alteration zone	Rock type	Alteration Type	Estimated T (°C)	Secondary minerals (vol%)
6R-2, 75-78	296.65	6	bgr alt	LP	low-T	50-100	phyll (7)
16R-1, 37-42	369.27	16a	bgr alt + h	ILF	low-T	50-100	sm (3), cel (1), Fe-oxhydr (3)
16R-1, 37-42	369.27	16b	bgr alt	ILF	low-T	50-100	sm (7)
37R-2, 119-121	502.79	37	bgr alt	ILF	low-T	50-100	sm (5)
52R-2, 23-28	602.43	52	bgr alt	L	low-T	50-100	sm (3)
66R-1, 14-17	710.54	66a	h	L	tr	50-100	Fe-oxhydr (4)
66R-1, 14-17	710.54	66b	bgr alt + h	L	tr	50-100	sm (2), cel (3), hsch (<1)
87R-2, 75-79	832.85	87	bgr alt	L	tr	50-100	sm/chl (10), hsch (<1)
102R-2, 1-4	927.99	102	bgr alt	L	tr	50-100	sm,/chl (7)
123R-1, 20-25	1032.30	123	bgr alt	LTZ	hydr	110-250	sm,/chl (4)
138R-2, 38-43	1105.83	138	bgr alt	SD	hydr	250-380	chl (7), tit (<1)
149R-1, 73-76	1157.60	149	vein	SD	hydr	250-380	amph(18), ep (10), anh (9), chl(4) qtz(4), zeol(>1), tit(1), cc(3), pyr(1)
150R-1, 26-29	1160.56	150a	bgr alt + h	SD	hydr	250-380	amph(12), alb(6), chl(2), tit(1)
150R-1, 26-29	1160.56	150b	bgr alt	SD	hydr	250-380	amph(6), alb(4), chl(2), tit(<1)
170R-1, 69-73	1252.49	170	bgr alt	SD	hydr	250-400	amph(5), chl(6), tit(<1)
189R-1, 58-61	1334.48	189	bgr alt	SD	hydr	250-400	amph(45), chl(2)
196R-1, 27-30	1363.97	196	bgr alt	gSD	grbl	300-480	amph(30)
207R-1, 0-4	1390.70	207	bgr alt	gSD	grbl	300-480	amph(40)
214R-2, 37-42	1412.72	214	bgr alt	G	hydr	300-480	amph(20), alb(7), chl(1), ep(1), prh(1)
220R-1, 48-52	1435.48	220	bgr alt	G	hydr	300-480	amph(20)
227R-2, 21-23	1470.21	227	bgr alt	gSD	grbl	300-480	amph(20)
231R-3, 0-7	1490.56	231	bgr alt	G	hydr	300-480	amph(25), chl(1)

Column 2: mbsf: meters below seafloor. Column 3: sample number used in this study. Column 4: alteration zones are either background alteration (bgr alt), background alteration associated with halo (bgr alt+h), individual halo (h) or vein. Column 5: LP: lava pond; ILF: inflated lava flows, L: ridge-axis lavas; LTZ: lithostratigraphic transition zone; SD: sheeted dike; gSD:granoblastic sheeted dike; G: gabbro. Column 6: low-T: low temperature; tr: transitional between low T and hydothermal alteration; hydr: hydrothermal; grbl: granoblastic. Column 7: temperatures estimated from oxygen isotope and fluid inclusion studies (Alt et al., 2010). Column 8: the values in brackets indicate the proportion of secondary minerals estimated from thin sections; phyll: phyllosilicate (see details in Alt and Laverne, 2006); sm: smectite; cel: celadonite; Fe-oxhydr: iron oxyhydroxide, hsch: hydroschorlomite (see details in Laverne et al., 2006); sm/chl: interlayered or mixed layered smectite/chlorite; chl: chlorite; amp: amphibole; ab: albite; ep: epidote; tit: titanite; prh: prehnite; anh: anhydrite; zeol: zeolite; qtz: quartz; pyr: pyrite; cc: calcite.

Table 2. Representative EMP chemical analyses of secondary minerals of samples from this study (ODP/IODP Hole 1256D). Complementary analyses from other samples (74R-2, 77R-1 and 89R-1) are also given.

Analysis run	B14	B14	B14	B7	B13	B9	B14	B14	B15	B15	B14	B14
Analysis #	85	32	67	46	115	331	41	126	16	19	26	30
Hole	1256D	1256D	1256D	1256D	1256D	1256D	1256D	1256D	1256D	1256D	1256D	1256D
Core-section	6R-2	37R-2	52R-2	74R-2	77R-1	89R-1	102R-2	123R-1	138R-2	138R-2	150R-1	150R-1
Interval (cm)	75-78	119-121	23-28	81-85	103-106	16-22	1-4	20-25	38-43	38-43	26-29	26-29
Mineral type	sm	sm	sm	sm	cel	sm	sm	chl	prh	chl	cc	chl
Mineral color	gr bwr	or	or	or		or	p brw					
SiO_2	33.18	47.63	47.00	40.00	48.42	41.88	46.14	31.00	41.20	28.33	0.00	29.00
TiO_2	0.05	0.35	0.16	0.06	0.03	0.00	0.17	0.00	0.00	0.06	0.00	0.00
Al_2O_3	10.43	3.42	7.67	8.78	6.35	8.01	5.57	13.58	22.64	15.53	0.00	17.92
CaO	1.08	1.70	2.49	4.69	0.77	2.66	2.68	0.66	22.10	0.84	59.11	0.22
Na_2O	0.31	0.36	0.13	0.20	0.20	0.06	0.14	0.03	0.01	0.06	0.03	0.03
K_2O	0.15	0.35	0.23	0.10	6.93	0.14	0.17	0.04	0.00	0.00	0.00	0.00
FeO	33.17	23.37	17.86	20.53	17.56	12.55	19.81	26.25	6.66	25.70	0.02	19.37
MgO	7.88	9.51	12.75	12.51	5.32	18.12	13.06	14.68	2.36	12.39	0.01	21.39
MnO	0.32	0.17	0.01	0.04	0.09	0.07	0.07	0.40	0.06	0.28	0.01	0.26
P_2O_5	0.02	0.00	0.04	0.00	0.02	0.05	0.00	0.02	0.01	0.00	0.05	0.00
Cl	0.01	0.08	0.05	0.07	0.29	0.10	0.02	0.05	0.00	0.03	0.01	0.01
F	0.19	0.00	0.05	0.00	0.00	0.04	0.00	0.03	0.06	0.00	0.00	0.01
ZnO	na	na	na	na	na	na	na	0.03	0.06	0.00	na	na
Cr_2O_3	0.03	0.00	0.00	0.04	0.11	0.00	0.01	na	na	na	0.00	0.03
ZrO_2	na	na	na	0.02	0.01	0.00	na	na	na	na	na	na
PbO	na	na	na	0.11	na	na	na	na	na	na	na	na
Total	86.83	86.94	88.44	87.17	86.09	83.69	87.84	86.75	95.15	83.24	59.24	88.23

sm: smectite-rich phyllosilicate; cel: celadonite-rich phyllosilicate; prh: prehnite; chl: chlorite; cc: calcite; ep: epidote; ab: albite; amp: amphibole; tit: titanite; phyll: phyllosilicate; tlc: talc; gr: green; brw: brown; or: orange; p: pale; int; na: not analyzed.

Table 2. (Continued).

Analysis run	B14	B14	B14	B14	B14	B14	B14	P6	B14	B15	B15	B15
Analysis #	27	22	176	170	167	164	205	37	210	33	67	45
Hole	1256D	1256D	1256D	1256D	1256D	1256D	1256D	1256D	1256D	1256D	1256D	1256D
Core-section	150R-1	150R-1	170R-1	170R-1	170R-1	170R-1	207R-1	220R-1	220R-1	227R-2	231R-3	231R-3
Interval (cm)	26-29	26-29	69-73	69-73	69-73	69-73	0-4	48-52	48-52	21-28	0-7	0-7
Mineral type	ep	ab	chl	amp	ab	tit	amp	amp	phyll	amp	amp	sm
Mineral color									dk gr		gr	dk brw
SiO_2	37.68	66.57	29.39	48.23	66.05	29.88	52.10	52.90	44.88	53.90	50.36	38.31
TiO_2	0.08	0.00	0.04	0.09	0.00	36.77	0.11	0.20	0.05	0.46	0.34	0.04
Al_2O_3	24.89	20.58	17.10	6.25	21.80	1.71	2.21	2.80	0.02	2.16	5.52	9.75
CaO	23.37	1.18	0.29	2.50	2.46	29.30	12.53	9.16	0.51	11.82	11.06	2.04
Na_2O	0.02	10.78	0.00	0.65	10.01	0.02	0.27	0.69	0.02	0.55	0.87	0.07
K_2O	0.00	0.11	0.03	0.00	0.00	0.00	0.00	0.07	0.01	0.02	0.05	0.06
FeO	10.91	0.07	20.79	27.33	0.08	1.45	16.74	15.14	14.22	12.45	17.04	23.59
MgO	0.23	0.01	19.42	11.72	0.00	0.00	13.53	16.64	29.17	16.43	13.11	13.07
MnO	0.38	0.00	0.15	0.42	0.01	0.00	0.38	0.32	0.16	0.19	0.30	0.09
P_2O_5	0.17	0.00	0.01	0.00	0.00	0.15	0.00	0.00	0.01	0.00	0.00	0.03
Cl	0.01	0.01	0.01	0.07	0.00	0.01	0.03	0.12	0.11	0.10	0.13	0.02
F	0.00	-0.09	0.06	0.00	0.00	0.42	0.10	0.00	0.00	0.00	0.04	0.10
ZnO	na	na	0.02	na	na	0.04	0.00	0.02	na	0.04	0.02	na
Cr_2O_3	0.00	0.00	na	0.03	0.00	na	na	0.00	0.00	na	na	0.00
ZrO_2	na	na	na	na	na	na	na	na	na	na	na	na
PbO	na	na	na	na	na	na	na	0.00	na	na	na	na
Total	97.74	99.33	87.20	97.28	100.42	99.76	98.01	98.05	89.15	98.10	98.85	87.19

Table 3. Abundance and isotope composition of hydrogen and carbon extracted during step-heating technique from samples of the Site 1256 (Leg 206, Expeditions 309, 312).

Spl #	H_2O (wt.%)	δD (‰)	CO_2 (ppm)					$\delta^{13}C$ (‰)	
			250ºC with O_2	900°C without O_2	1170ºC without O_2	1170ºC with O_2	Total	250ºC	(900+1170)ºC
6	0.58	-64.2	95	1429	222	L.b.	1746	-20.9	-25.0
16a	0.61	-57.2	188	955	126	L.b.	1269	-26.5	-26.6
16b	0.66	-53.6	261	2511	89	L.b.	2823	n.a	-25.4
37	0.32	-56.3	96	471	102	L.b.	784	-22.7	-23.7
52	0.34	-63.7	142	918	46	L.b.	1126	-21.0	n.a
66a	0.65	-46.9	22	1376	186	39	1643	-21.3	-22.6
66b	0.51	-51.5	162	1652	80	L.b.	1895	-24.6	-21.3
87	0.83	-36.4	121	1272	97	L.b.	1594	-17.2	-21.7
102	0.43	-40.6	162	570	63	79	874	-22.7	-22.0
123	1.75	n.a	364	1456	193	L.b.	2409	n.a	n.a
123	1.83	-42.5	170	1751	403	11	2335	-26.4	-23.6
138	1.65	-28.9	101	1626	140	37	1839	-26.3	-19.9
149	3	-40.4	611	20230	10515	2898	34254	n.a	-10.9
150a	2.14	-25.5	149	2410	61	L.b.	2629	-25.4	-14.9
150b	1.75	-38.8	70	848	64	L.b.	973	-24.3	n.a
170	1.57	-25.1	87	1106	48	9	1209	-27.5	n.a
189	1.65	-30.5	59	502	100	L.b.	644	-28.4	-22.4
196	0.79	-41.7	57	489	43	2	564	n.a	-22.7
207	0.87	-43.1	111	974	90	L.b.	1158	n.a	-20.9
214	0.89	-55.0	57	593	62	L.b.	676	n.a	-22.1
220	0.91	-35.2	55	812	66	L.b.	945	-30.4	-17.3
227	0.7	-47.1	20	690	70	12	775	-28.1	-23.0
231	0.83	-40.0	20	524	93	L.b.	652	-25.4	-21.9
Blank*			15	33	29	46			

n.a =non analyzed

L.b.= Less than blank.

* Average blank was expressed in ppm for each step by dividing blank amount (in μmol) by average sample weight (~200 mg)

Table 4. CO_2 extracted from carbonates after H_3PO_4 attack at 80ºC.

Spl #	CO_2 (μmol)	Total CO_2 (ppm)	$\delta^{13}C$ (‰)
16a	0.97	38	n.d.
16a	1.32	58	n.d.
37	0.2	7	n.d.
66a	0.61	26	n.d.
123	0.74	106	-15.2
149	83.9	18312	-4.5
220	2.6	161	n.d.

Table 5. Results of the modeling for C and H speciation in rocks from Hole 1256D (see main text for details).

Spl #	Depth (mbsf)	C_{OC}/C_{tot} (1) (molar ratio)	C_{OC}/C_{tot} (2) (molar ratio)	C_{OC} (3) (μmol/g)	$(H_{OC})_{max}$ (4) (μmol/g)	$(H_{OC})_{min}$ (5) (μmol/g)	H_{OC}/H_{tot} (6) (molar ratio)
6	296.65	0.93	0.94	37.4	149.6	74.8	0.23
16a	369.27	1.00	1.00	28.8	115.4	57.7	0.17
16b	369.27	0.95	0.96	61.4	245.4	122.7	0.33
37	502.79	0.87	0.89	15.9	63.8	31.9	0.18
66a	710.54	0.82	0.85	31.9	127.4	63.7	0.18
66b	710.54	0.76	0.81	34.7	138.9	69.4	0.25
87	832.85	0.78	0.82	29.7	118.8	59.4	0.13
102	927.99	0.79	0.83	16.5	66.2	33.1	0.14
123	1032.30	0.86	0.89	47.2	188.8	94.4	0.09
138	1105.83	0.70	0.75	31.5	126.0	63.0	0.07
150a	1160.56	0.47	0.57	33.8	135.4	67.7	0.06
189	1334.48	0.81	0.85	12.4	49.5	24.8	0.03
196	1363.97	0.82	0.86	11.0	43.9	21.9	0.05
207	1390.70	0.74	0.79	20.8	83.2	41.6	0.09
214	1412.72	0.80	0.84	12.8	51.4	25.7	0.05
220	1435.48	0.58	0.66	14.1	56.4	28.2	0.06
227	1470.21	0.84	0.87	15.3	61.3	30.7	0.08
231	1490.56	0.78	0.82	12.2	48.7	24.4	0.05

(1) Fraction of organic carbon calculated assuming C corresponds to a mixing between carbonates with $\delta^{13}C$=-4.5‰ and organic carbon with $\delta^{13}C$=-26.6‰.
(2) Fraction of organic carbon calculated assuming C corresponds to a mixing between carbonates with $\delta^{13}C$=+0.4‰ and organic carbon with $\delta^{13}C$=-26.6‰.
(3) Organic C content calculated from C_{org}/C_{tot} (2) and measured CO_2 concentration in bulk rock (given in Table 3).
(4) Maximum H content contained in organic compounds calculated for C/H molar ratio in alkane of 0.25.
(5) Minimum H content contained in organic compounds calculated for C/H molar ratio in alkane of 0.5.
(6) Maximum molar fraction of H present in organic compounds calculated from $(H_{org})_{max}$.

Table 6. Average C content in altered oceanic crust

Lithological unit	Thickness (km)	CO_2 wt%		
		Ctot [a]	Corg [b]	Ccarb [c]
Volcanic Section	0.6	2.00	0.12	1.87
Transition Zone	0.2	0.58	0.17	0.43
Sheeted Dikes	1.2	0.07	0.07	0
Gabbros	5	0.02	0.02	0
Mean crust	7	0.21	0.04	0.17

[a] Ctot: total carbon, including carbonates and organic compounds - data from Alt and Teagle (1999)
[b] Corg: organic compounds - determined from the average in Hole 1256 samples, except for the gabbros where values of 0.02 was assumed from Alt and Teagle data (1999). This assumption relies on the high number of analyses from Alt and Teagle and the fact that organic carbon content cannot be higher than total carbon content.
[c] Ccarb: calculated from the difference Ctot - Corg

FIGURE 1

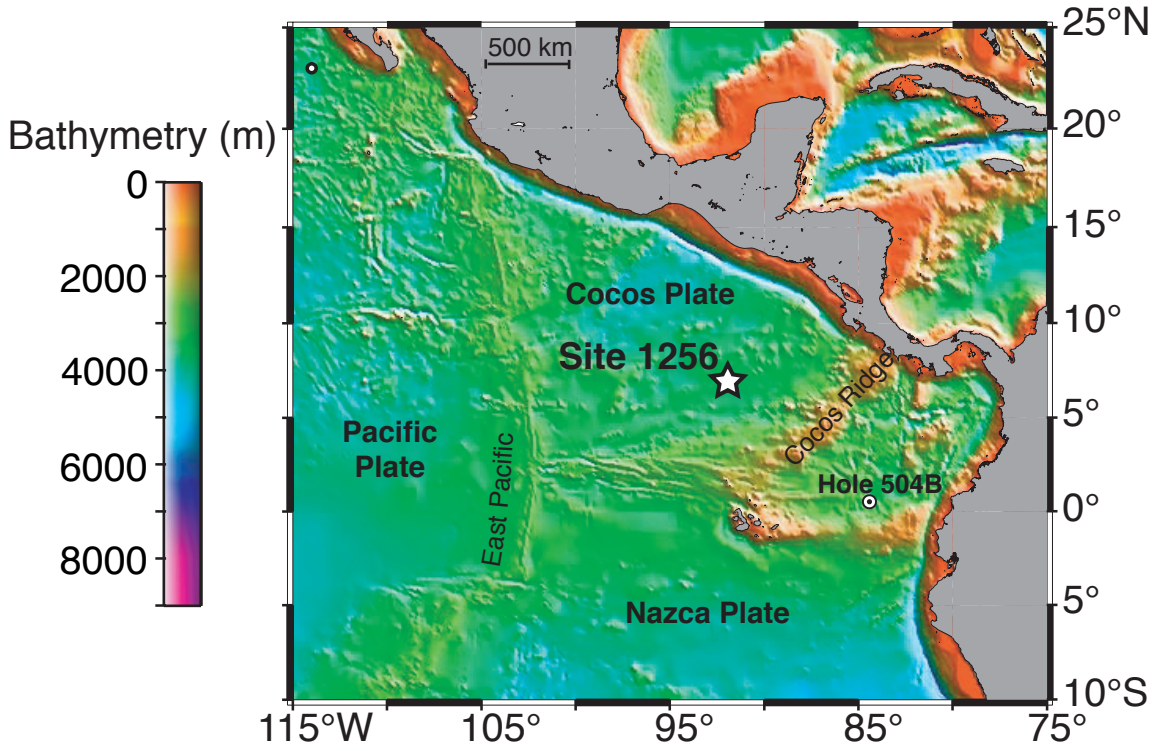

FIGURE 2

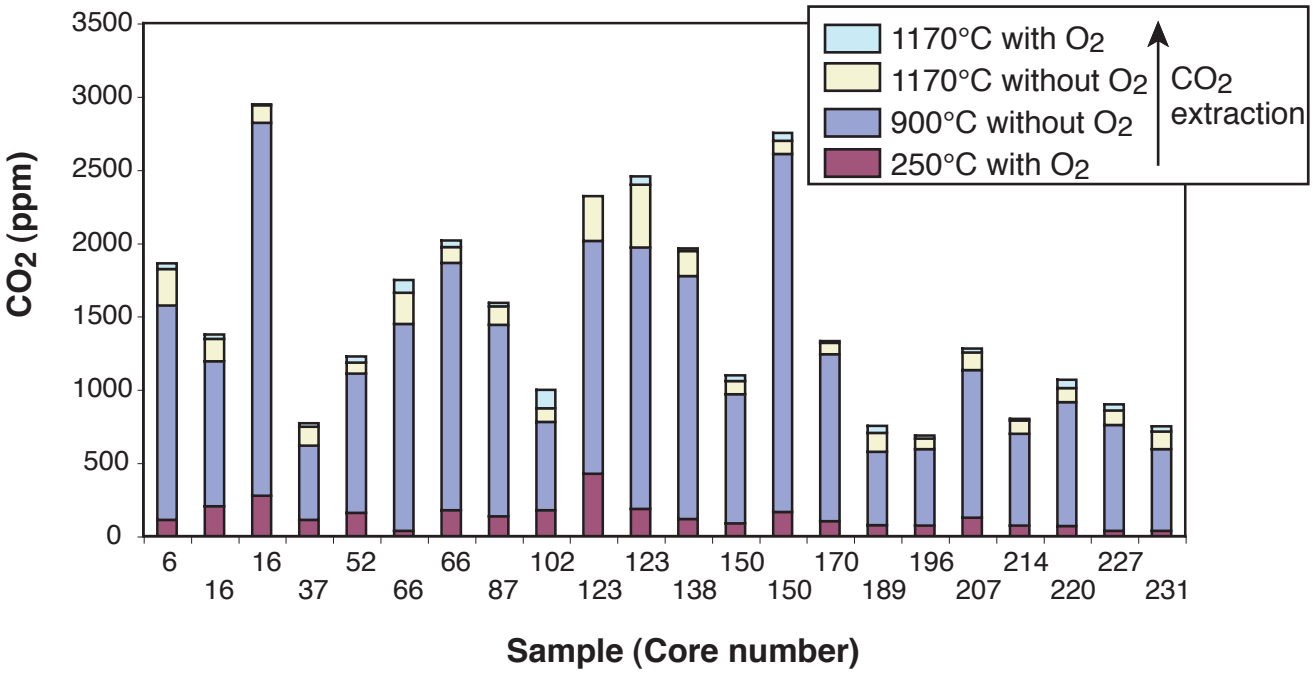

FIGURE 3

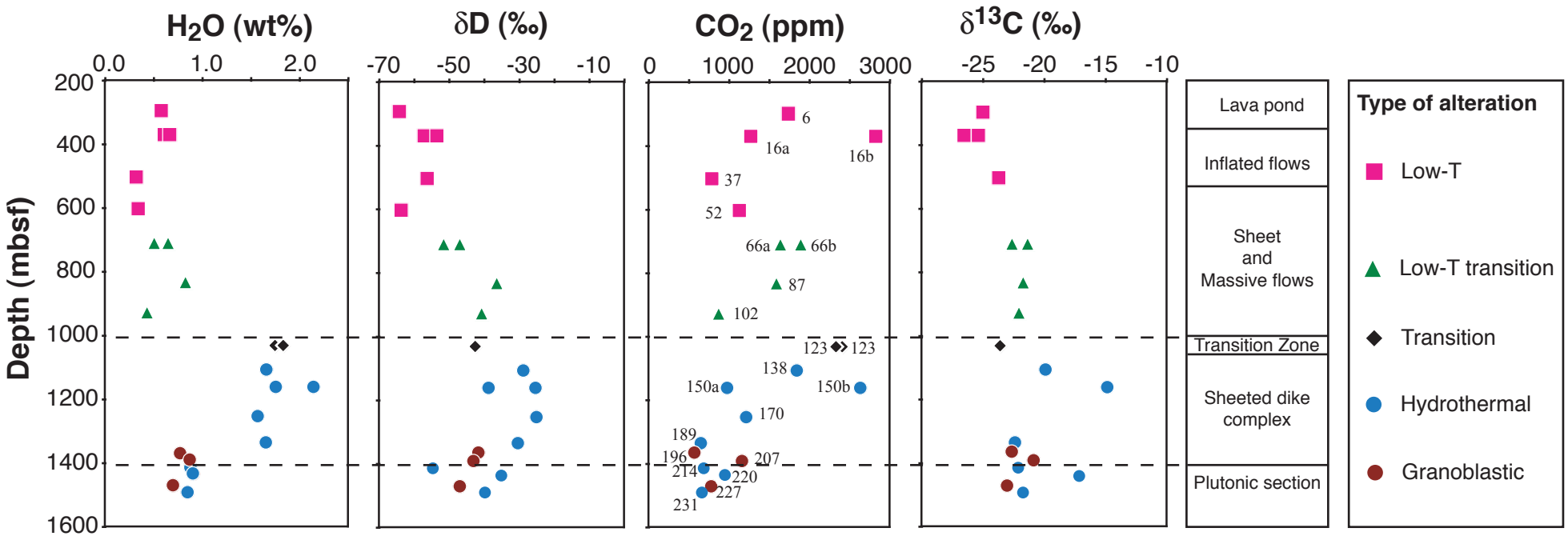
H2O (wt%)
δD (‰)
CO2 (ppm)
δ13C (‰)
0.0
1.0
2.0
-70
-50
-30
-10
0
1000
2000
3000
-25
-20
-15
-10
Depth (mbsf)
200
400
600
800
1000
1200
1400
1600
6
16a
16b
37
52
66a
66b
87
102
123
123
138
150a
150b
170
189
196
207
214
220
227
231
Lava pond
Inflated flows
Sheet and Massive flows
Transition Zone
Sheeted dike complex
Plutonic section
Type of alteration
Low-T
Low-T transition
Transition
Hydrothermal
Granoblastic

FIGURE 4

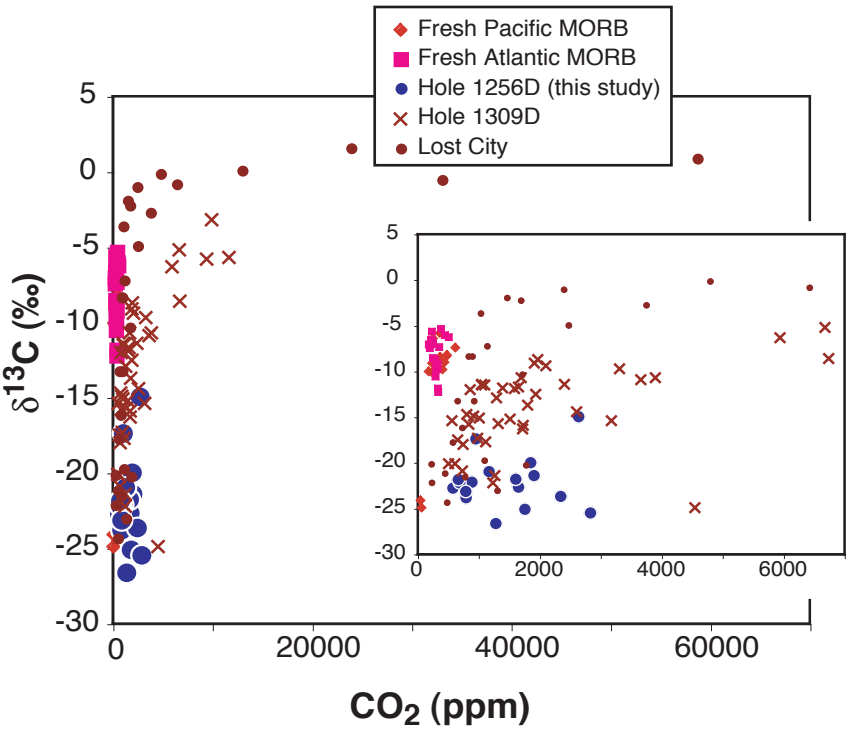

FIGURE 5

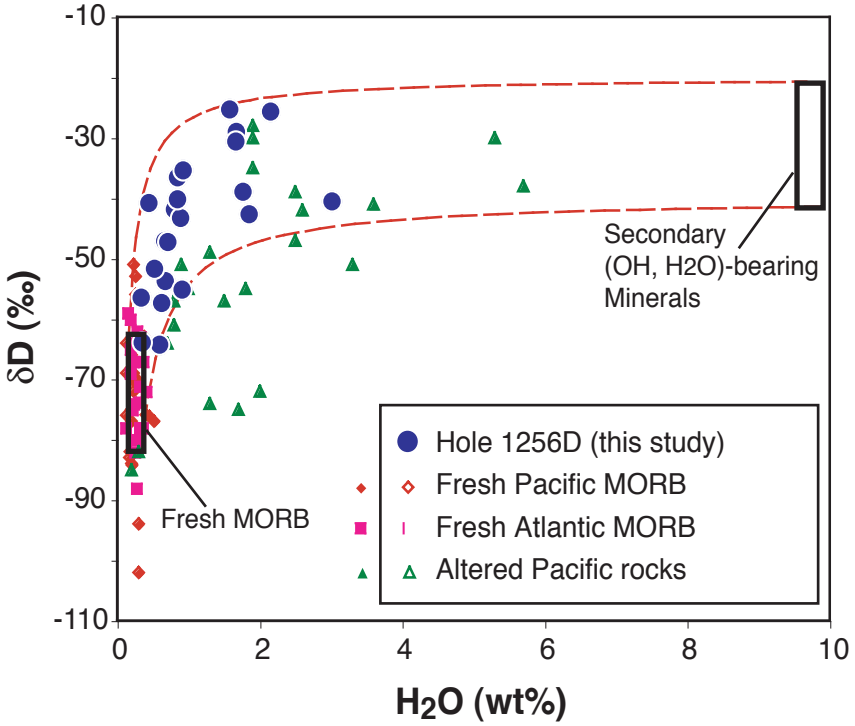

FIGURE 6

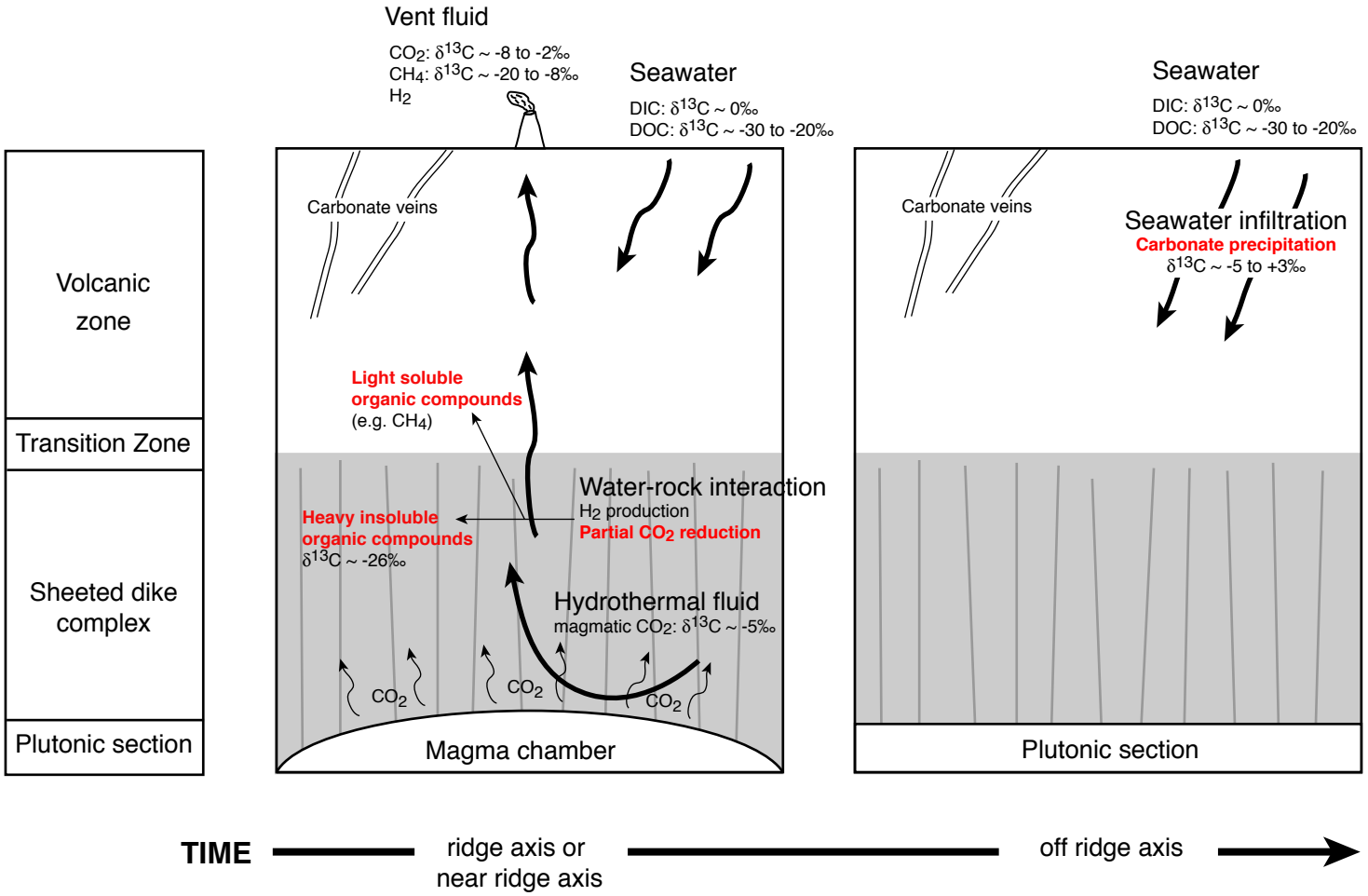
Vent fluid
CO_2: $\delta^{13}C$ ~ -8 to -2‰
CH_4: $\delta^{13}C$ ~ -20 to -8‰
H_2
Seawater
DIC: $\delta^{13}C$ ~ 0‰
DOC: $\delta^{13}C$ ~ -30 to -20‰
Seawater
DIC: $\delta^{13}C$ ~ 0‰
DOC: $\delta^{13}C$ ~ -30 to -20‰
Volcanic zone
Transition Zone
Sheeted dike complex
Plutonic section
Carbonate veins
Carbonate veins
Seawater infiltration
Carbonate precipitation
$\delta^{13}C$ ~ -5 to +3‰
Light soluble organic compounds
(e.g. CH_4)
Water-rock interaction
H_2 production
Partial CO_2 reduction
Heavy insoluble organic compounds
$\delta^{13}C$ ~ -26‰
Hydrothermal fluid
magmatic CO_2: $\delta^{13}C$ ~ -5‰
CO_2
CO_2
CO_2
Magma chamber
Plutonic section
TIME
ridge axis or near ridge axis
off ridge axis